High-fidelity Simulations of ArcJets

Nagi N. Mansour

November 14th, 2019

ARCHeS team:
Jeremie Meurisse,
Magnus Haw,
Joey Schulz,
Sergio Fraile,
Sander Visser,

Stardust entry
Jan 15, 2006

Interaction Heating Facility (IHF)

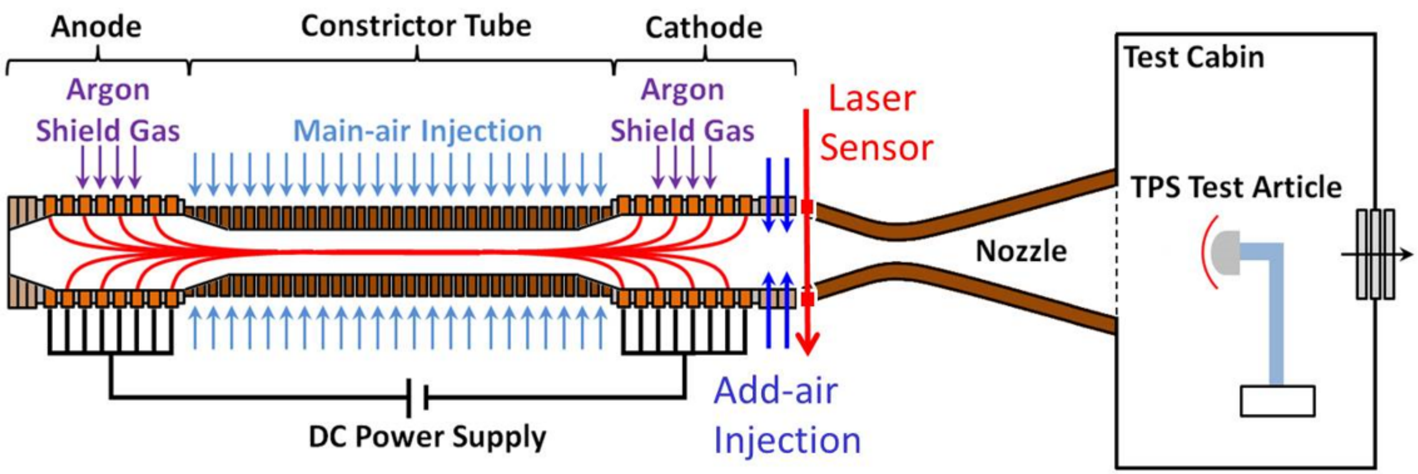

Arc Jet Experiment on meteorites

5 second exposure

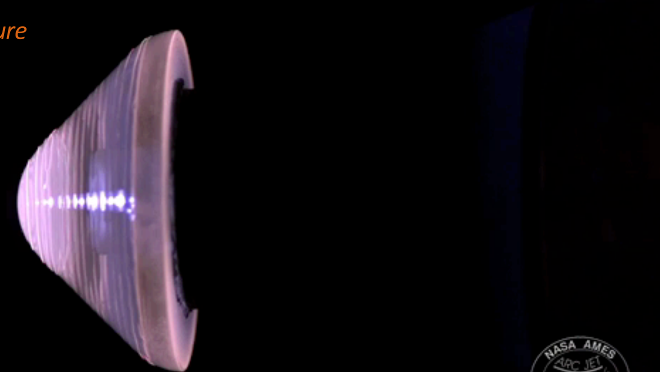

Pure Silica

5 second exposure

Terrestrial Basalt

3 second exposure

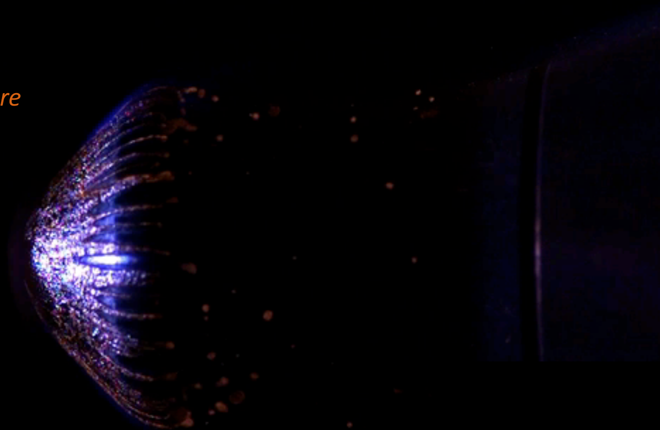

Campo del Cielo Iron Meteorite

2 second exposure

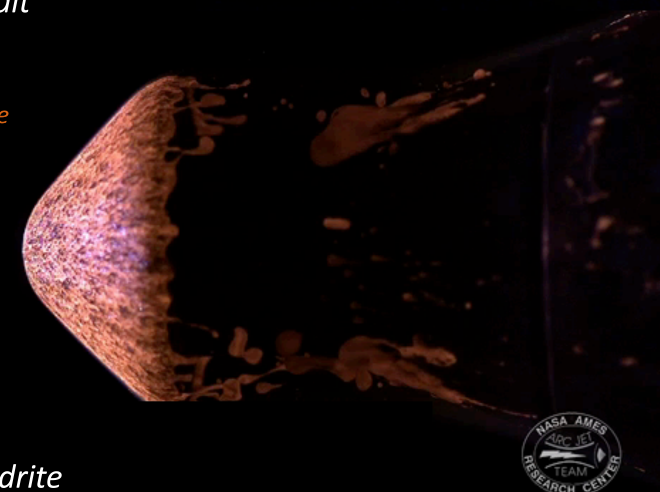

Tamdakht H5 Chondrite

NASA Entry Vehicles / Missions Supported by Ames

Entry Systems and Technology Division

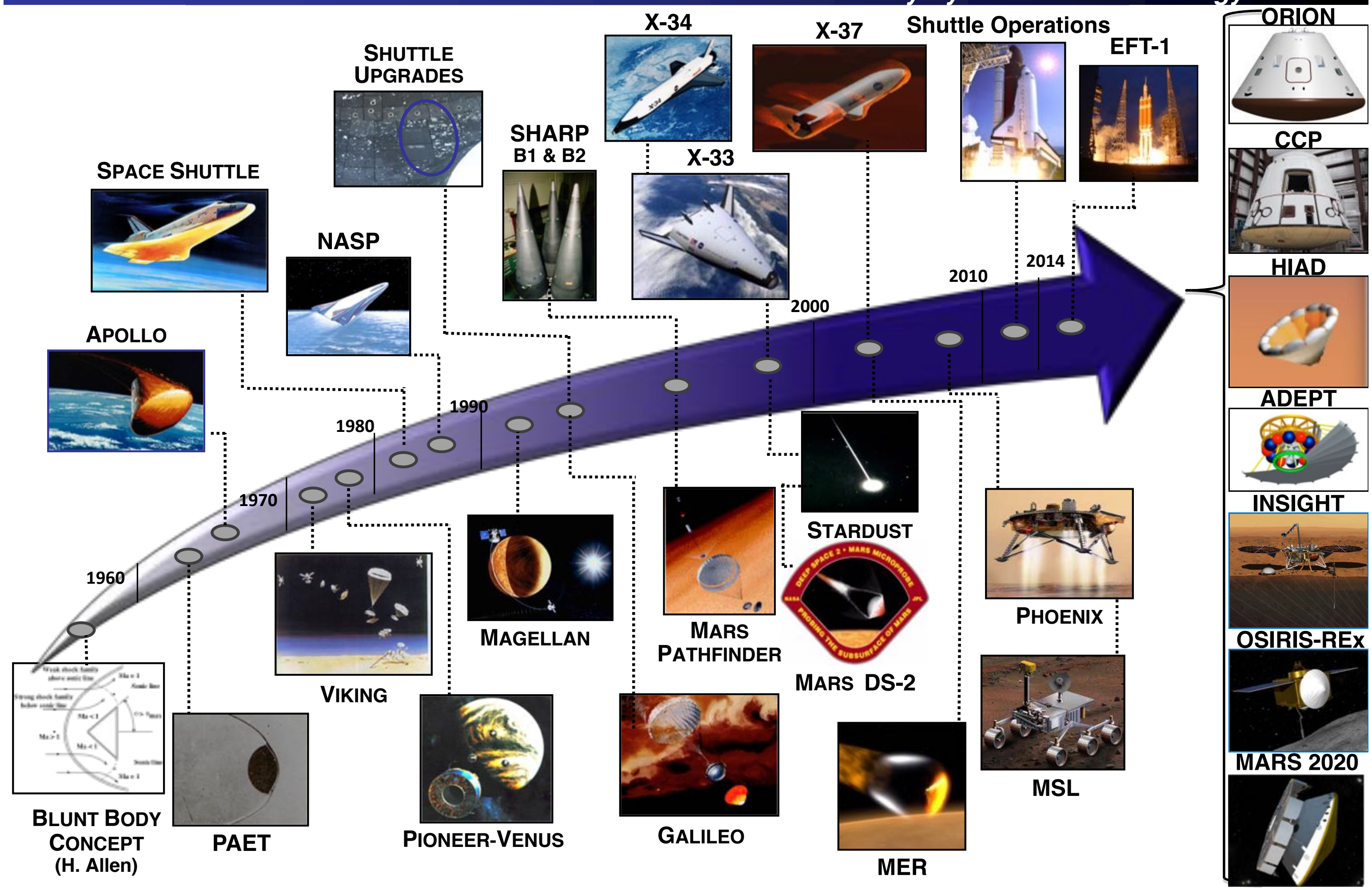

Ames Arc Jet Complex

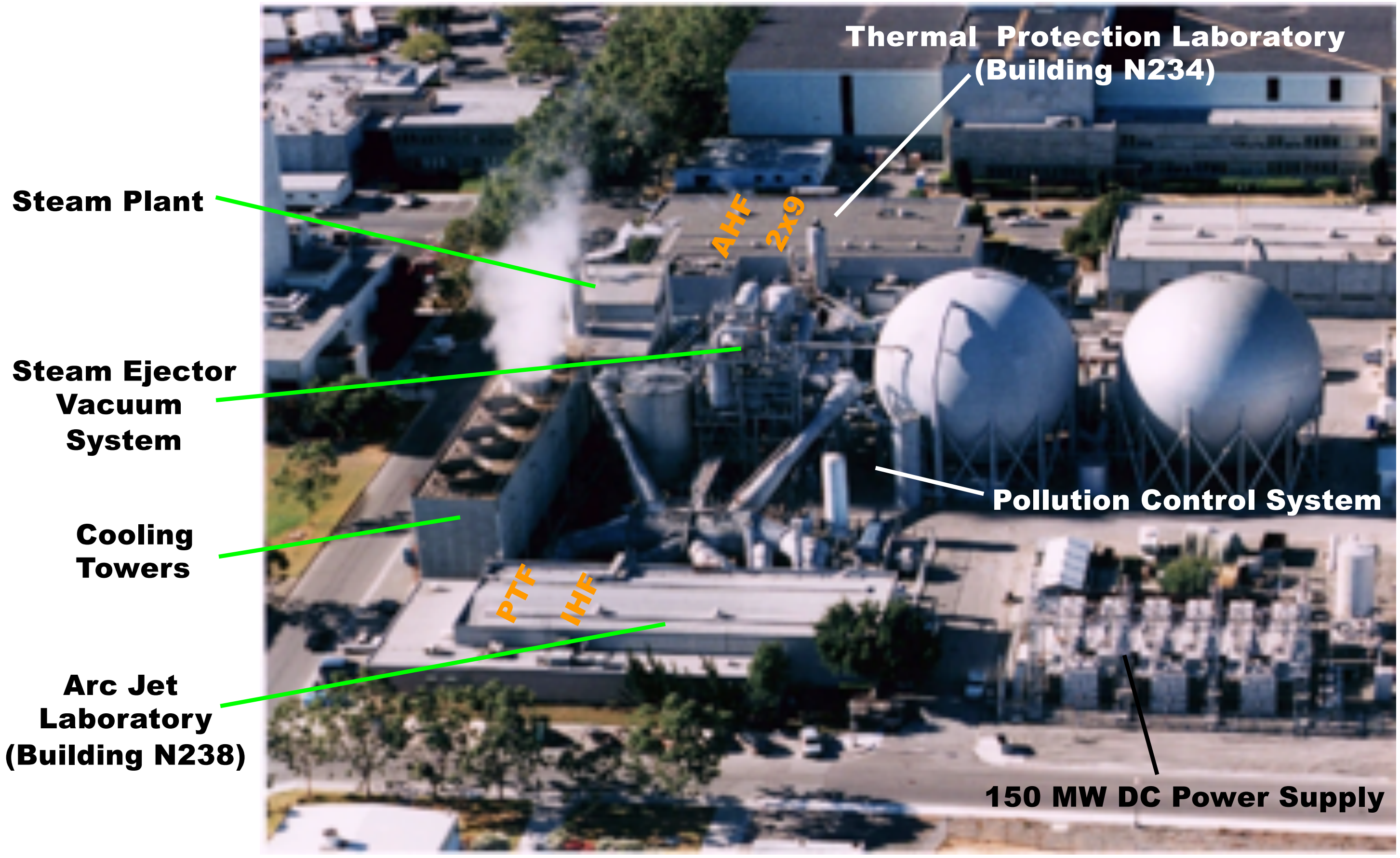

High enthalpy arc-jets

Looking down the column

Looking along the column

Test chamber

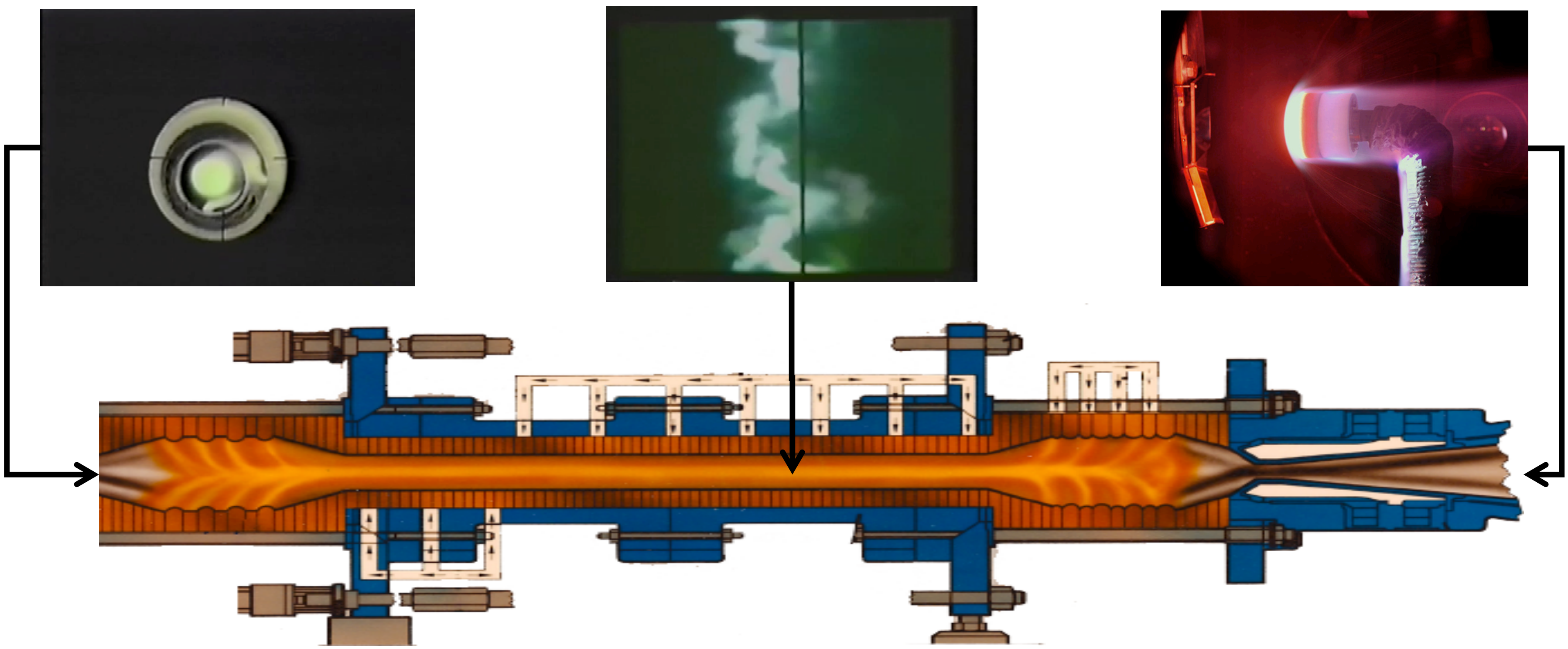

Needed: Capability to perform realistic simulations

Bruce Walter Arc Heater visualization

1D study of the mini-Arc
(with J.B. Scoggins & J. Jimenez-Miro)

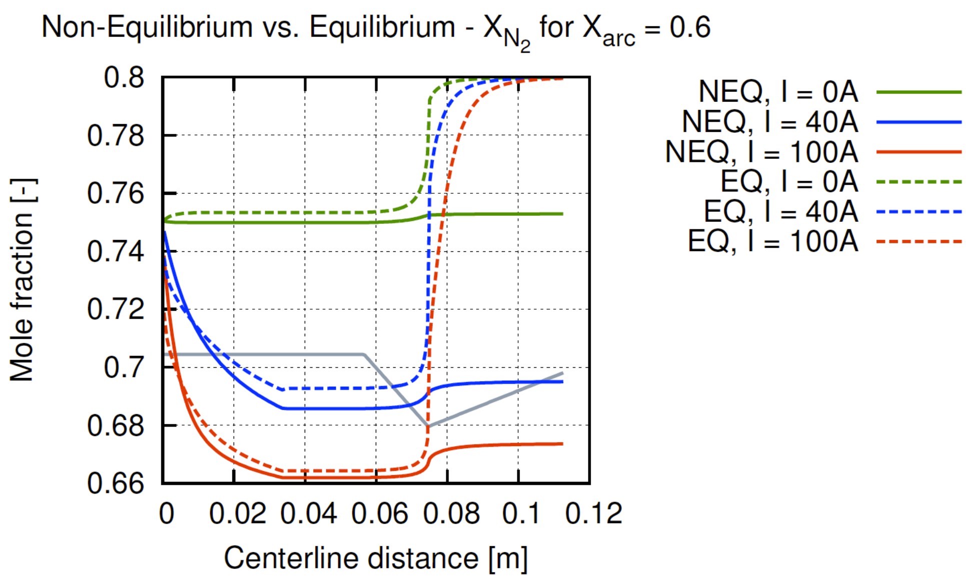

(a) Mole fraction of N_2.

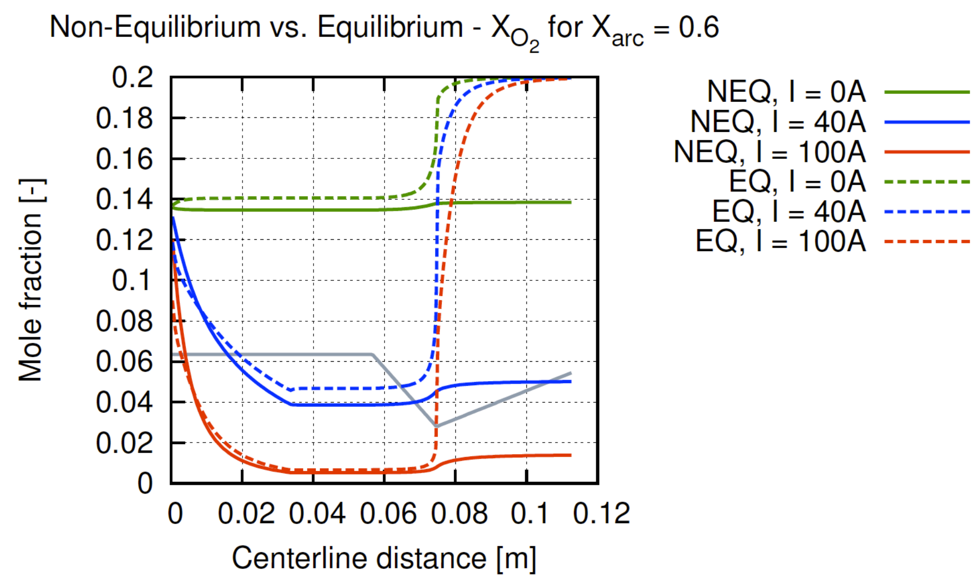

(b) Mole fraction of O_2.

1D study of the mini-Arc

(Note from J.B. Scoggins)

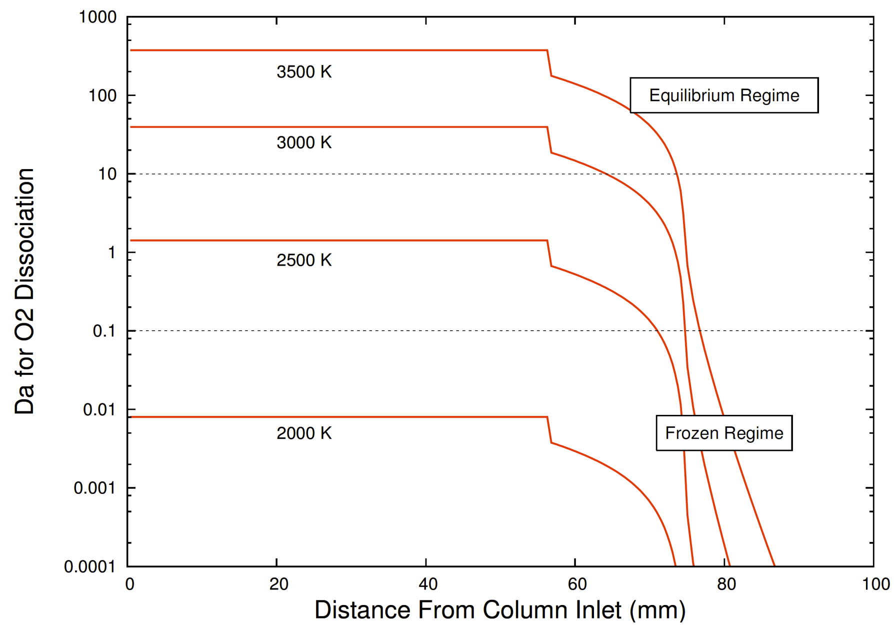

Figure 1: Damkohler number associated with the O2 dissociation reaction for different inlet temperatures.

⇒ Equilibrium formulation for applications of interest (high pressure ~ 9atm, high temperature ~10,000 K)

Interaction Heating Facility (IHF)

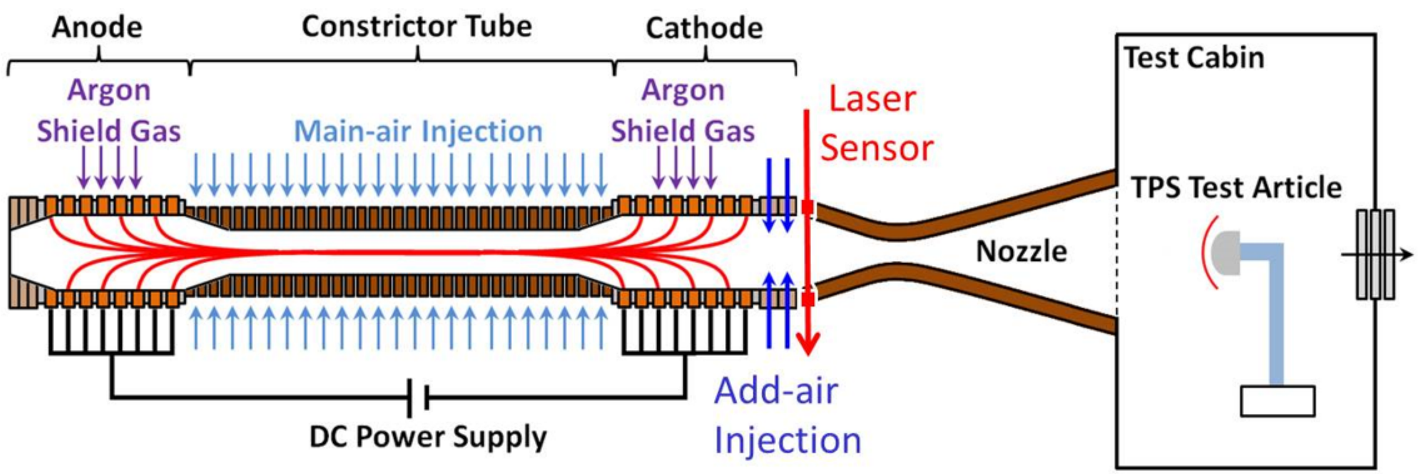

Characteristics:

- High pressure
- High temperature
- Variable Air/Ar mixture
- Strong Imposed voltage drop (constant current)
- Ballast at the electrodes to ensure uniform current
- External **B** to force current to rotate around the electrode

Interaction Heating Facility (IHF)

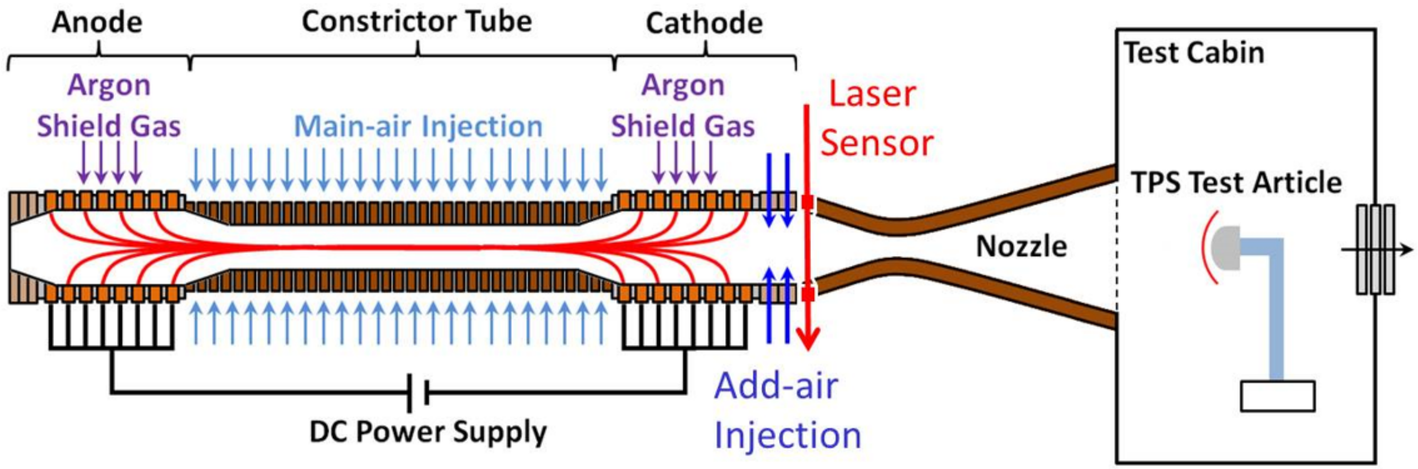

Characteristics:

- High pressure
- High temperature
- Variable Air/Ar mixture
- Strong Imposed voltage drop (constant current)
- Ballast at the electrodes to ensure uniform current
- External **B** to force current to rotate around the electrode

Compressible Navier-Stokes Equations:
Equilibrium formulation with variable elemental fraction

$$\frac{\partial \rho_i}{\partial t} + \boldsymbol{\nabla} \cdot (\rho_i \boldsymbol{u} + \boldsymbol{F}_i^d) = 0 \qquad i \in [1, N_e]$$

$$\frac{\partial \rho \boldsymbol{u}}{\partial t} + \boldsymbol{\nabla} \cdot (\rho \boldsymbol{u}\boldsymbol{u}) = -\boldsymbol{\nabla} p + \boldsymbol{\nabla} \cdot \bar{\bar{\tau}} + \boldsymbol{J} \times \boldsymbol{B}$$

$$\frac{\partial \rho E}{\partial t} + \boldsymbol{\nabla} \cdot (\rho H \boldsymbol{u}) + \boldsymbol{\nabla} \cdot (\boldsymbol{q}_d) = \boldsymbol{\nabla} \cdot (\bar{\bar{\tau}} \cdot \boldsymbol{u} - \boldsymbol{q}) + \sigma |\boldsymbol{E}|^2 + \boldsymbol{u} \cdot (\boldsymbol{J} \times \boldsymbol{B}) - \boldsymbol{\nabla} \cdot \boldsymbol{q}_{rad}$$

$$\rho = \sum_i^{N_e} \rho_i = \sum_k^{N_s} \rho_k \qquad Z_i = \frac{\rho_i}{\rho} \qquad Z_i^x = \frac{\rho_i \; M^m}{\rho \; M_i^m} \qquad i \in [1, N_e]$$

$$H = E + \frac{p}{\rho} = e + \frac{|\boldsymbol{u}|^2}{2} + \frac{p}{\rho}$$

Compressible Navier-Stokes Equations:

Equilibrium formulation with variable elemental fraction

$$\boldsymbol{F}_i^d = \rho_i \boldsymbol{v}_i = \left(\frac{\partial F_i^d}{\partial p}\right) \boldsymbol{\nabla} p + \left(\frac{\partial F_i^d}{\partial T}\right) \boldsymbol{\nabla} T + \sum_j^{N_e} \left(\frac{\partial F_i^d}{\partial Z_j^x}\right) \boldsymbol{\nabla} Z_j^x \qquad i,j \in [1, N_e]$$

$$\left(\frac{\partial F_i^d}{\partial p}\right) = -\sum_k^{N_s} \rho_k \frac{M_i^m}{M_k^m} \nu_{ki} \sum_l^{N_s} D_{kl} \left(\frac{\partial X_l}{\partial p} + \frac{X_l - Y_l}{p}\right) \qquad i,j \in [1, N_e] \ \ \& \ \ k,l \in [1, N_s]$$

$$\left(\frac{\partial F_i^d}{\partial T}\right) = -\sum_k^{N_s} \rho_k \frac{M_i^m}{M_k^m} \nu_{ki} \sum_l^{N_s} D_{kl} \left(\frac{\partial X_l}{\partial T} + \frac{\kappa_l^r}{T}\right) \qquad i,j \in [1, N_e] \ \ \& \ \ k,l \in [1, N_s]$$

$$\left(\frac{\partial F_i^d}{\partial Z_j^x}\right) = -\sum_k^{N_s} \rho_k \frac{M_i^m}{M_k^m} \nu_{ki} \sum_l^{N_s} D_{kl} \left(\frac{\partial X_l}{\partial Z_j^x}\right) \qquad i,j \in [1, N_e] \ \ \& \ \ k,l \in [1, N_s]$$

Transport properties from MUTATION++

References

V. Giovangigli, Multicomponent Flow Modeling, Birkhäuser, Boston, 1999

J.B. Scoggins, T.E. Magin, Development of Mutation++: multicomponent thermodynamic and transport property library for ionized plasmas written in C++, AIAA Pap. 2966 (2014)

Tabulated Air/Ar mixtures Interpolation assuming n_O/n_N stays constant

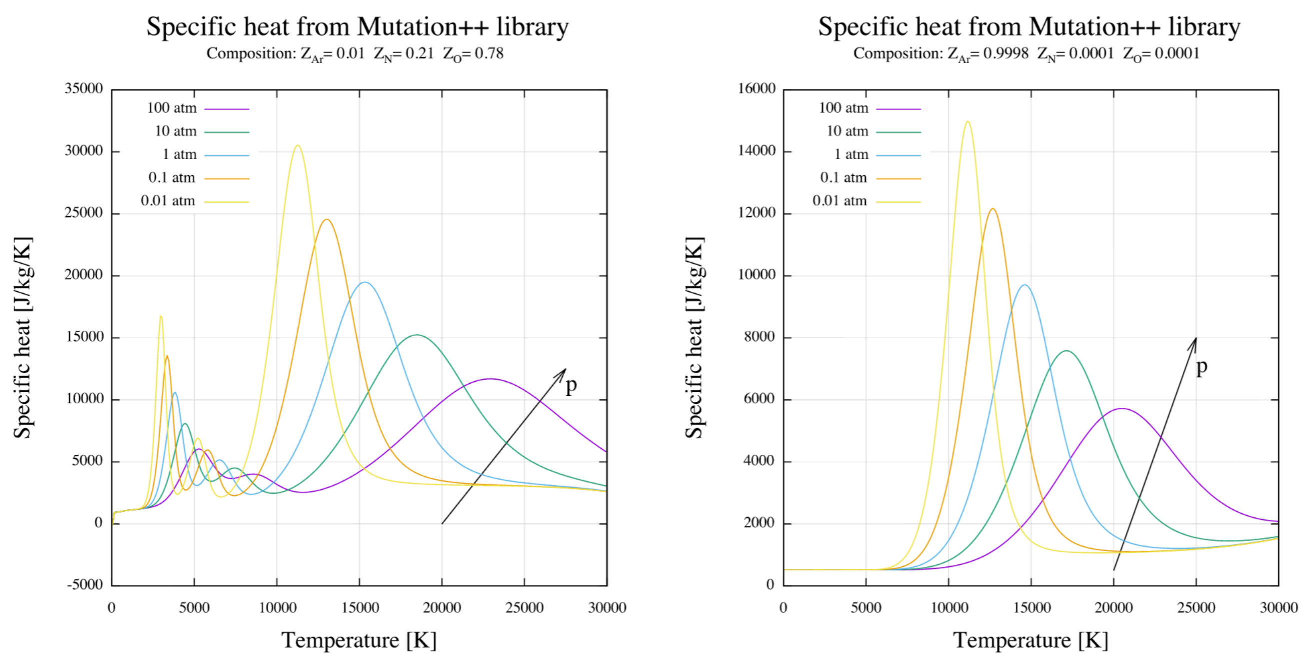

Figure 12: Specific heat from *Mutation++* library for air (left) and Argon (right) in function of p and T.

Interaction Heating Facility (IHF)

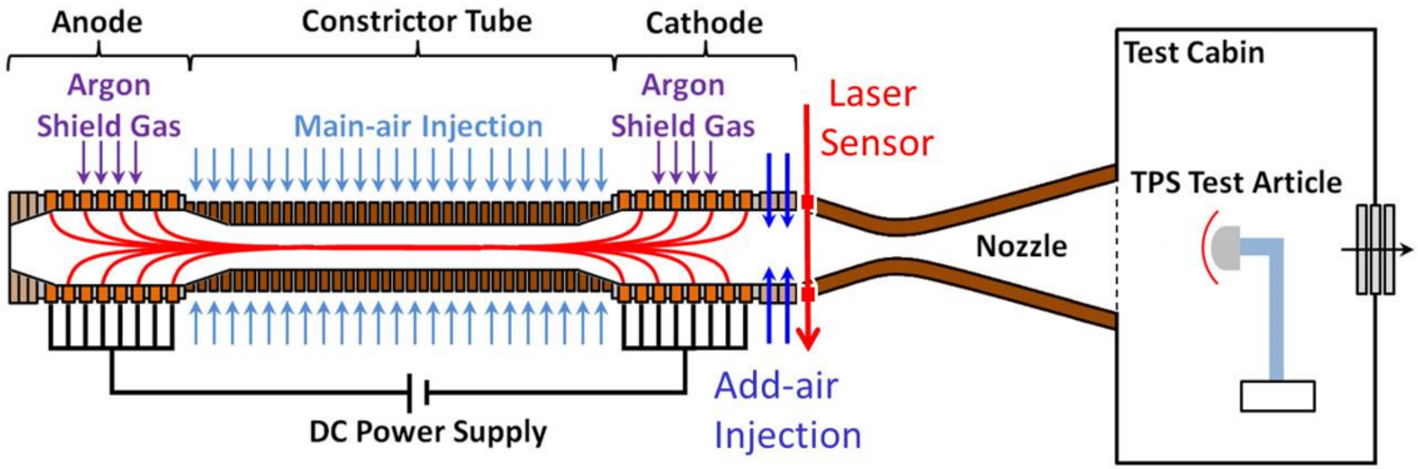

Characteristics:

- High pressure
- High temperature
- Variable Air/Ar mixture
- Strong Imposed voltage drop (constant current)
- Ballast at the electrodes to ensure uniform current
- External **B** to force current to rotate around the electrode

MHD approximation

$$\boldsymbol{\nabla} \times \boldsymbol{B} = \mu_0 \boldsymbol{J}$$

$$\text{Set } \boldsymbol{B} = \boldsymbol{\nabla} \times \boldsymbol{A}$$

$$\sigma \frac{\partial \boldsymbol{A}}{\partial t} - \frac{1}{\mu_0} \nabla^2 \boldsymbol{A} - \sigma \boldsymbol{u} \times (\boldsymbol{\nabla} \times \boldsymbol{A}) + \sigma \boldsymbol{\nabla} \psi = 0$$

where ψ is a Coulomb potetntial determined so that:

$$\boldsymbol{\nabla} \cdot \boldsymbol{A} = 0$$

Splitting the Electric field

$$\boldsymbol{E} = \boldsymbol{E}_{imp} + \boldsymbol{E}_g$$

$$\boldsymbol{E}_{imp} = -\boldsymbol{\nabla}\phi_{imp}$$

$$\boldsymbol{\nabla} \cdot (\boldsymbol{J}_{imp}) = 0$$

$$\boldsymbol{\nabla} \cdot (\boldsymbol{J}_{imp}) = 0 \quad \Rightarrow \quad \boxed{\boldsymbol{\nabla} \cdot (-\sigma \boldsymbol{\nabla}\phi_{imp}) = 0}$$

Boundary conditions

Anode

$$-\sigma \boldsymbol{\nabla}\phi_{imp} = \text{Const.}$$

$$\phi_{imp} = \text{Const.}$$

Cathode

$$\phi_{imp} = 0$$

Interaction Heating Facility (IHF)

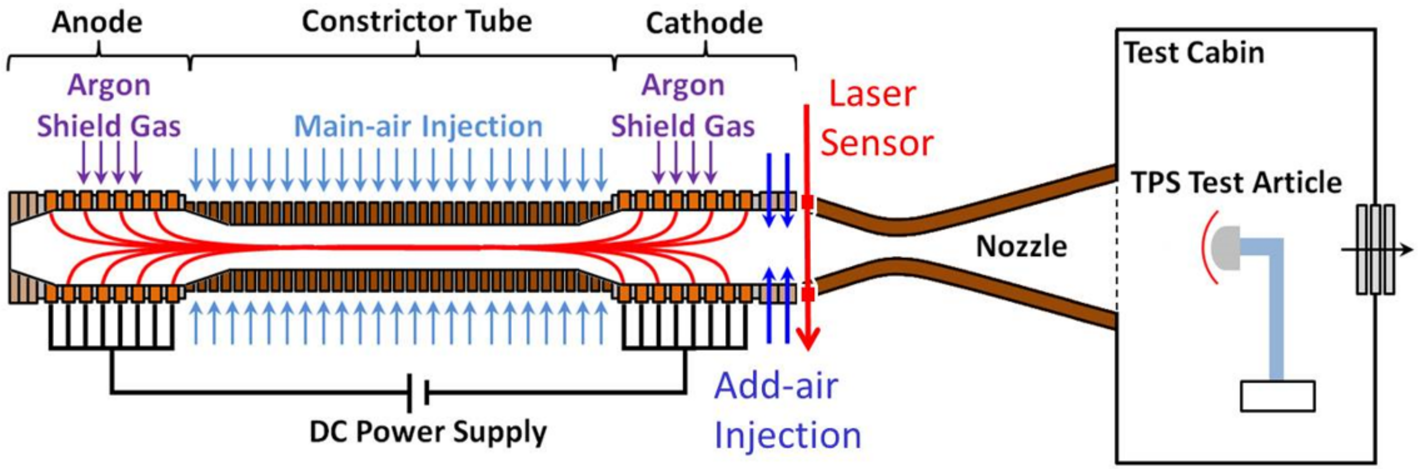

Characteristics:

- High pressure
- High temperature
- Variable Air/Ar mixture
- Strong Imposed voltage drop (constant current)
- Ballast at the electrodes to ensure uniform current
- External **B** to force current to rotate around the electrode

Balast boundary condition

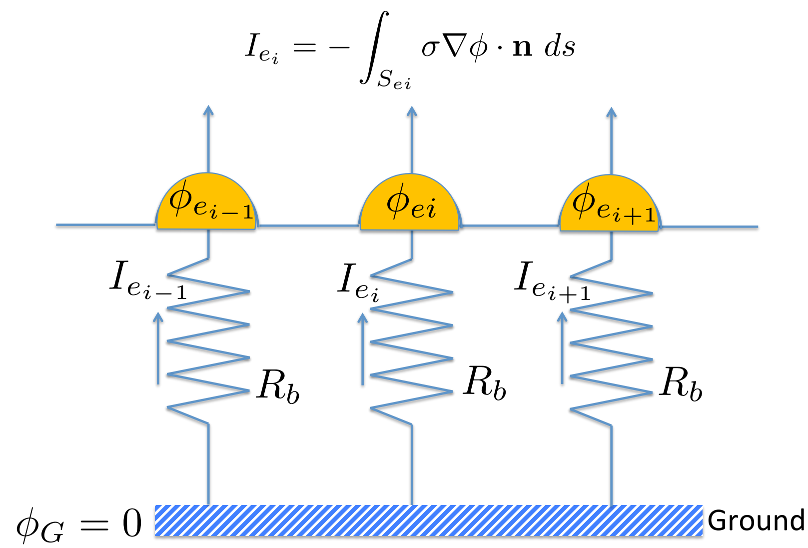

$$-I^c_{e_i} = \int_{S^c_{e_i}} \sigma \; \nabla\phi \cdot \mathbf{n} \; ds = \frac{1}{R_b}(\phi_{e_i} - \phi_G)$$

$$\phi^n_{e_i} = \phi_G - R_b \int_{S^c_{e_i}} \sigma \; \nabla\phi^{n-1} \cdot \mathbf{n} \; ds$$

Interaction Heating Facility (IHF)

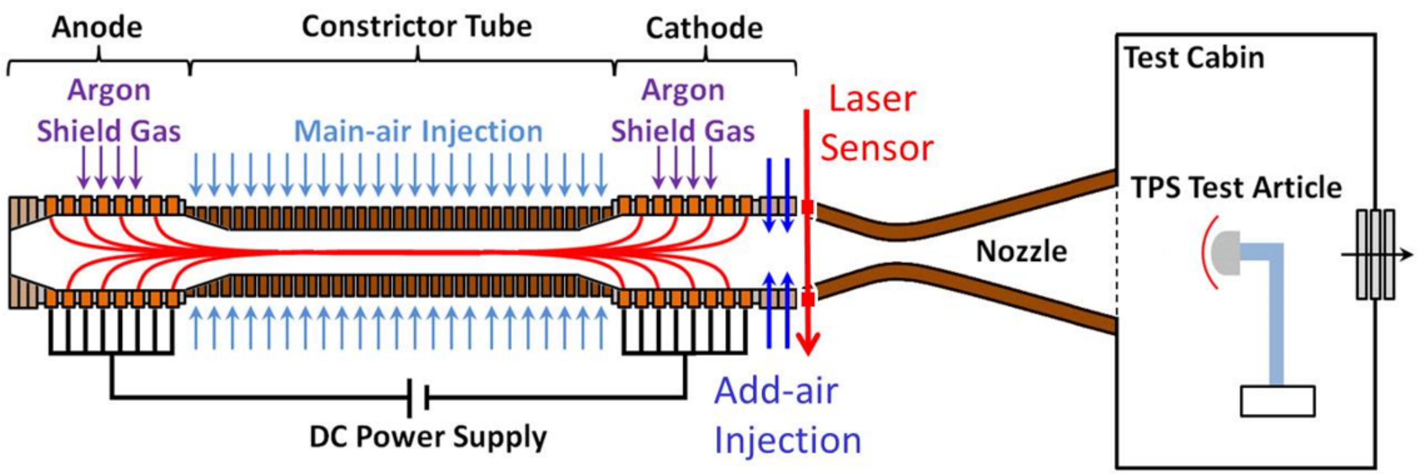

Characteristics:

- High pressure
- High temperature
- Variable Air/Ar mixture
- Strong Imposed voltage drop (constant current)
- Ballast at the electrodes to ensure uniform current
- External **B** to force current to rotate around the electrode

Electromotive force

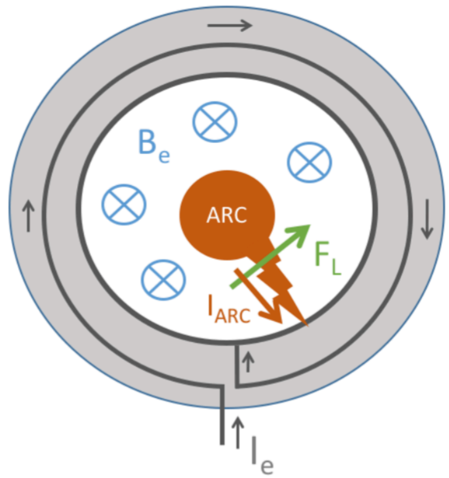

Figure 6: Electrode with Internal Magnetic Drive.

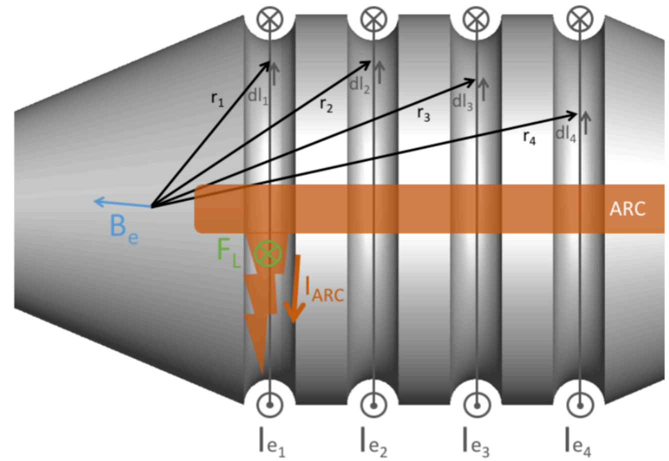

Figure 7: B_e for an anode with 4 electrodes.

Biot-Savart

$$\boldsymbol{B_e} = \sum_{i}^{N_e} \frac{\mu_0 I_{e_i}}{4\pi} \oint \frac{\boldsymbol{dl_i} \times \boldsymbol{r_i}}{|\boldsymbol{r_i}|^3}$$

Interaction Heating Facility (IHF)

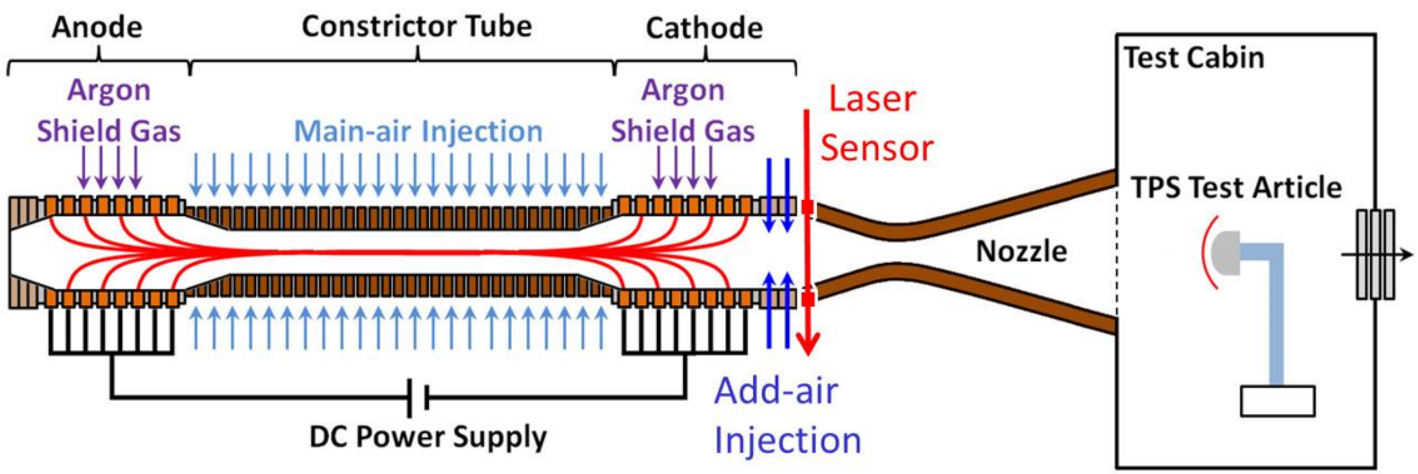

Characteristics:

- High pressure
- High temperature
- Variable Air/Ar mixture
- Strong Imposed voltage drop (constant current)
- Ballast at the electrodes to ensure uniform current
- External **B** to force current to rotate around the electrode

Radiative transport

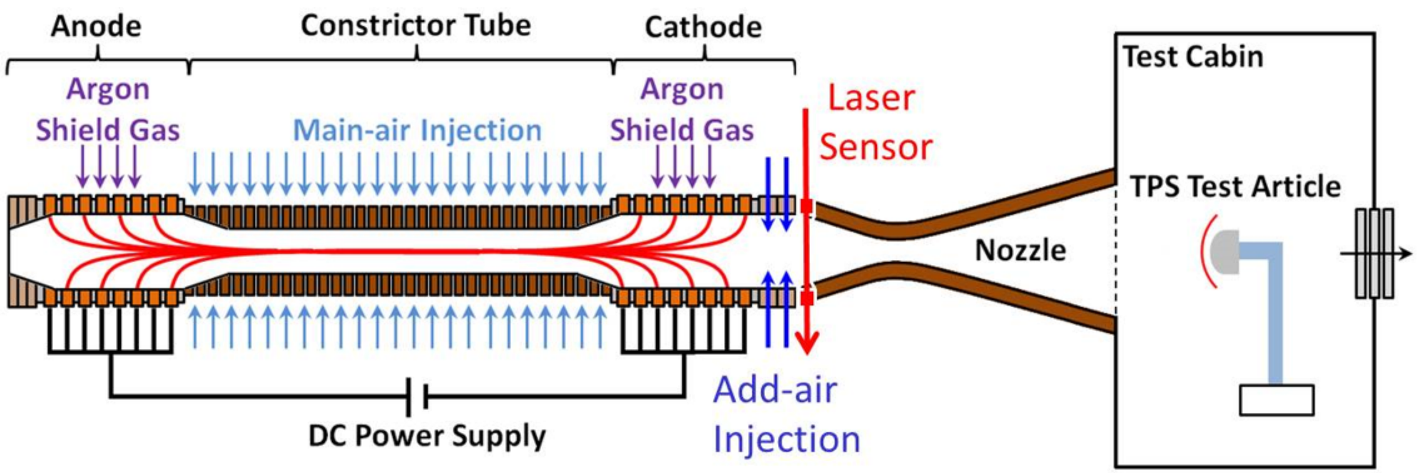

$$\boldsymbol{\Omega} \cdot \nabla I_\nu = \kappa_\nu (S_\nu - I_\nu)$$

$$\boldsymbol{Q} = \int_\nu \int_\Omega I_\nu \vec{\Omega} \, d\Omega \, d\nu$$

$$\nabla \cdot \boldsymbol{Q} = \int_\nu \int_\Omega \kappa_\nu (S_\nu - I_\nu) \, d\Omega \, d\nu$$

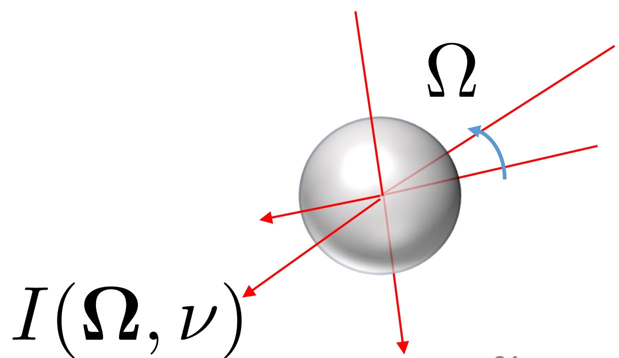

Radiation transfer Computing the line-by-line (LBL) opacity of a mixture

$$\kappa_{mix} = X\,\kappa_{air} + Y\,\kappa_{argon}$$

$$X = \frac{A}{B\,(\frac{C-D}{E} + \frac{A}{B})} \quad \text{and} \quad Y = \frac{C-D}{E\,(\frac{C-D}{E} + \frac{A}{B})} = 1 - X$$

$$A = \sum n(N, N^+, N_2, N_2^+, O, O^+, O_2, O_2^+, NO, NO^+)_{mix}$$

$$B = \sum n(N, N^+, N_2, N_2^+, O, O^+, O_2, O_2^+, NO, NO^+)_{air}$$

$$C = \sum n(Ar, Ar^+)_{mix} \qquad D = \sum n(Ar, Ar^+)_{air} \qquad E = \sum n(Ar, Ar^+)_{argon}$$

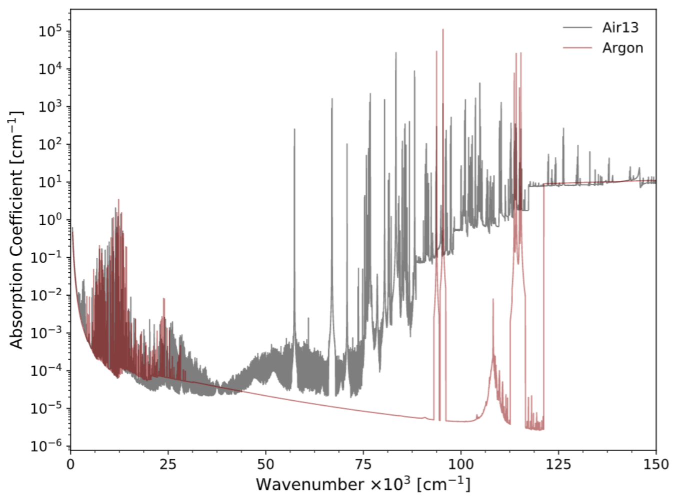

Fig. 1: Spectral absorption coefficients for LTE air and argon at 10,000 K and 1 atm

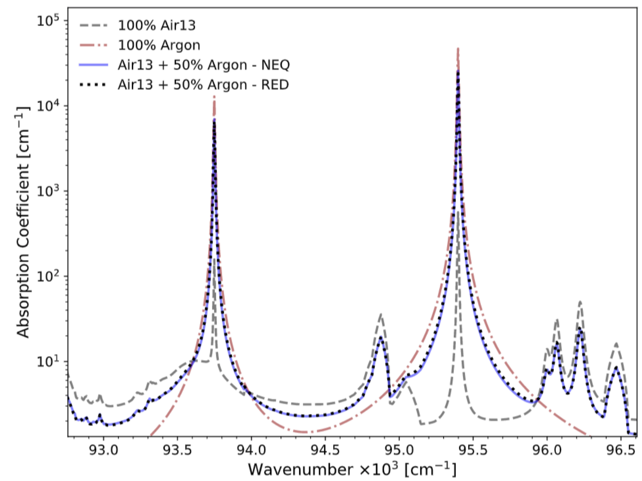

Fig. 2: LBL absorption coefficient for a mixture with a mol fraction of 0.5 air + 0.5 argon at 15,000 K and 10 atm computed with the reduced model (RED) vs NEQAIR (NEQ)

Radiation transfer Binning the opacity into tables

$$\frac{\partial I_\lambda(\widehat{\boldsymbol{n}}, s)}{\partial s} = \kappa_\lambda(s)\left[B_\lambda(T) - I_\lambda(\widehat{\boldsymbol{n}}, s)\right]$$

$$\frac{\partial}{\partial s}\bar{I}_b = \overline{\kappa_\lambda B_\lambda}|_b - \overline{\kappa_\lambda I_\lambda}|_b \quad \text{where,} \quad \bar{f}_b = \int_{\lambda_1}^{\lambda_2} f_\lambda \, d\lambda$$

$$\overline{\kappa_\lambda I_\lambda}|_b \approx \tilde{\kappa}_b \, \bar{I}_b$$

Planck-averaged $$\tilde{\kappa}_b = \kappa_{P_b} = \frac{\int_{\lambda_1}^{\lambda_2} \kappa_\lambda \, B_\lambda \, d\lambda}{\int_{\lambda_1}^{\lambda_2} B_\lambda \, d\lambda}$$

Rosseland-averaged $$\tilde{\kappa}_b = \kappa_{R_b} = \frac{\int_{\lambda_1}^{\lambda_2} \frac{\partial B_\lambda}{\partial T} \, d\lambda}{\int_{\lambda_1}^{\lambda_2} \frac{1}{\kappa_\lambda} \frac{\partial B_\lambda}{\partial T} \, d\lambda}$$

Blended-average $$\tilde{\kappa}_b = \kappa_{PR_b} = \sqrt{\kappa_{P_b} \, \kappa_{R_b}}$$

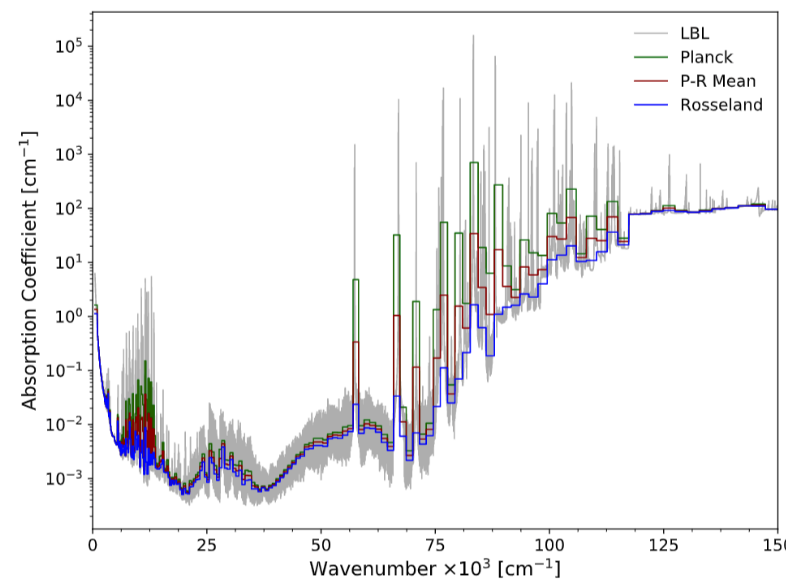

(b) 250 Bands

Fig. 3: Comparison of the different band averaging models for air at 10,000 K and 10 atm

Radiative transport

$$\int_V \boldsymbol{\Omega} \cdot \nabla \bar{I}_b \, dV = \int_V \nabla \cdot (\boldsymbol{\Omega} \bar{I}_b) \, dV = \int_S \bar{I}_b \boldsymbol{\Omega} \cdot d\boldsymbol{S} = \int_V \kappa_\nu (\bar{S}_b - \bar{I}_b) \, dV$$

$$\sum_k \bar{I}_{b,k}(\Omega_i) \boldsymbol{\Omega} \cdot \Delta \boldsymbol{S}_k = \bar{\kappa}_b (\bar{S}_{b,c} - \bar{I}_{b,c}(\Omega)) \, V_c$$

up-winding

$$\sum_{k \in \boldsymbol{\Omega_i} \cdot \Delta \boldsymbol{S}_k < 0} \bar{I}_{b,k}(\Omega_i) \boldsymbol{\Omega} \cdot \Delta \boldsymbol{S}_k + \sum_{k \in \boldsymbol{\Omega} \cdot \Delta \boldsymbol{S}_k > 0} \bar{I}_{b,c}(\Omega) \boldsymbol{\Omega} \cdot \Delta \boldsymbol{S}_k = \bar{\kappa}_{b,c} (\bar{S}_{b,c} - \bar{I}_{b,c}(\Omega_i)) \, V_c$$

$$\bar{I}_{b,c}(\Omega_i) = \frac{-\sum_{k \in \boldsymbol{\Omega} \cdot \Delta \boldsymbol{S}_k < 0} \bar{I}_{b,k}(\Omega_i) \boldsymbol{\Omega} \cdot \Delta \boldsymbol{S}_k + \bar{\kappa}_{b,c} \bar{S}_{b,c} V_c}{\sum_{k \in \vec{\Omega} \cdot \Delta \boldsymbol{S}_k > 0} \boldsymbol{\Omega} \cdot \Delta \boldsymbol{S}_k + \bar{\kappa}_{b,c} V_c}$$

Radiative transport

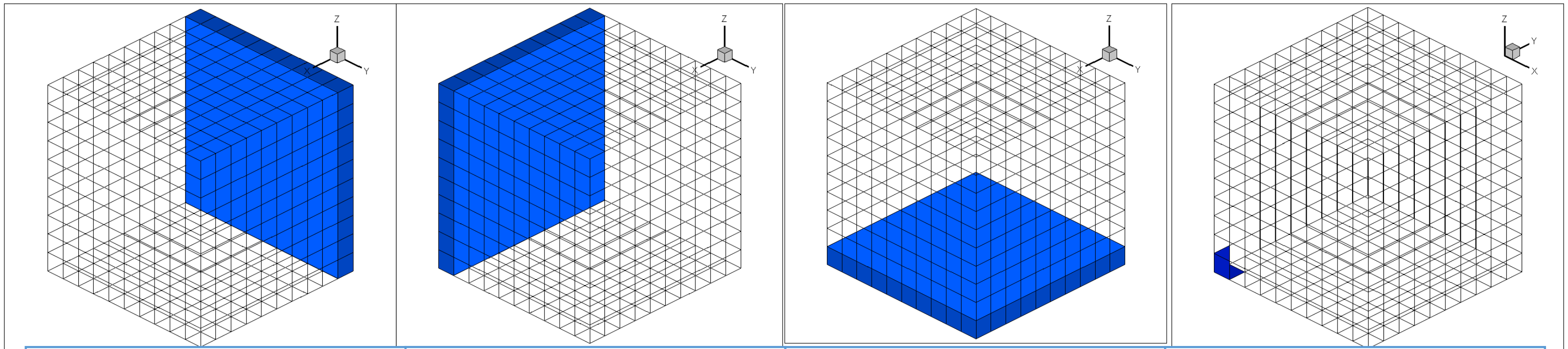

$\mathbf{\Omega} = (1,0,0)$	$\mathbf{\Omega} = (0,1,0)$	$\mathbf{\Omega} = (0,0,1)$	$\mathbf{\Omega} = (1,1,1)$

Animation Courtesy: Alejandro Alvarez

$$\boldsymbol{Q} = \int_{\nu} \int_{\Omega} I(\mathbf{\Omega}, \nu)\ d\Omega\ d\nu \approx \sum_{b} \sum_{\Omega_i} w_i \bar{I}_b(\Omega_i)$$

ARC Heater Simulator (ARCHeS)

ARCHeS

MHD	*Surface current interaction*
3D radiation	*Surface response*
Air-Ar chemistry	*Swirling and ballast BC*

ARC Heater Simulator (ARCHeS)

OpenFOAM

Modern
Modular
Finite-volume
IO, MPI
Turbulence

ARCHeS

MHD
3D radiation
Air-Ar chemistry

Surface current interaction
Surface response
Swirling and ballast BC

ARC Heater Simulator (ARCHeS)

OpenFOAM

Modern
Modular
Finite-volume
IO, MPI
Turbulence

ARCHeS

MHD
3D radiation
Air-Ar chemistry
Surface current interaction
Surface response
Swirling and ballast BC

Pointwise

Complex
Geometry
Generation

ARC Heater Simulator (ARCHeS)

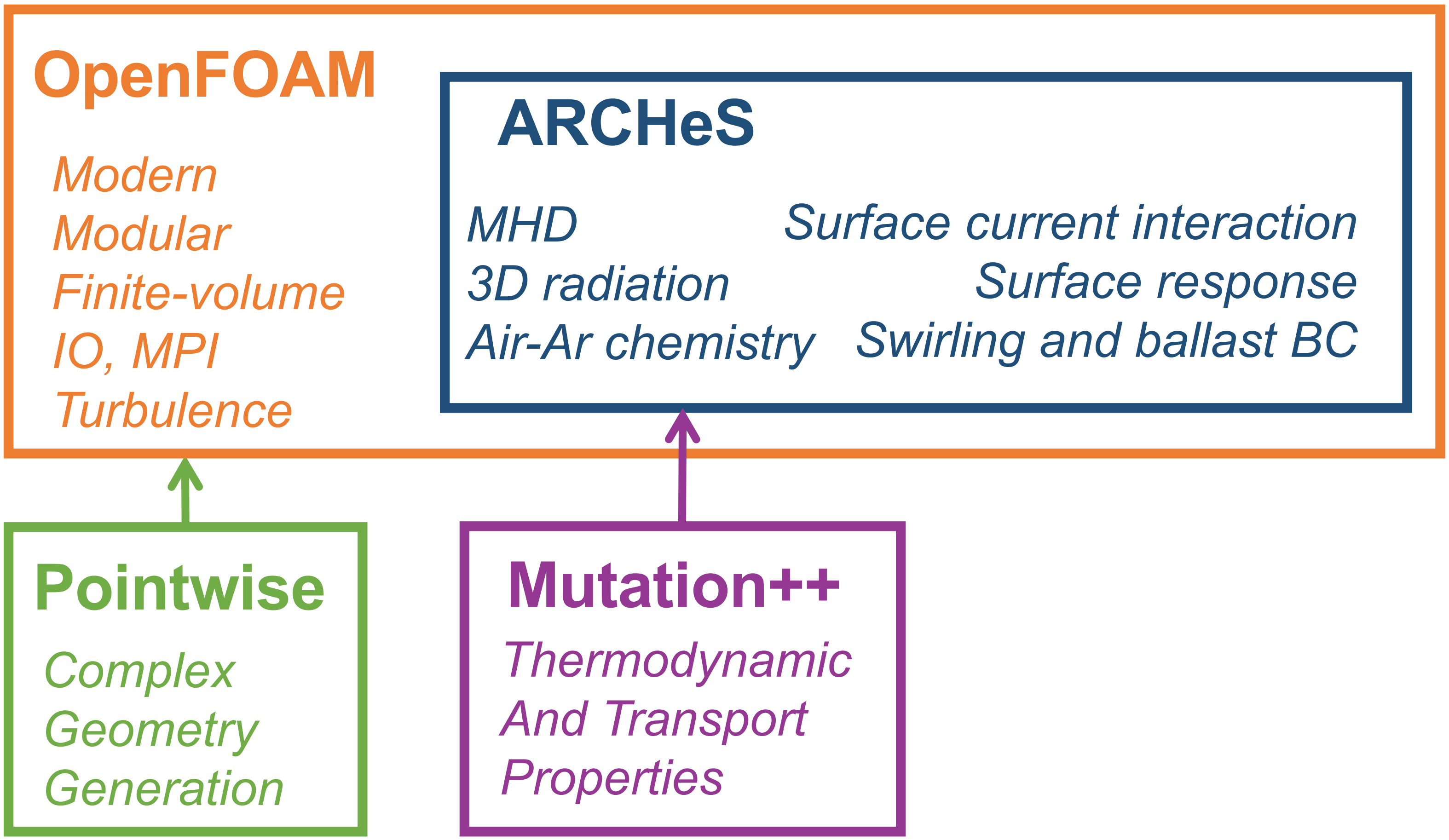

ARC Heater Simulator (ARCHeS)

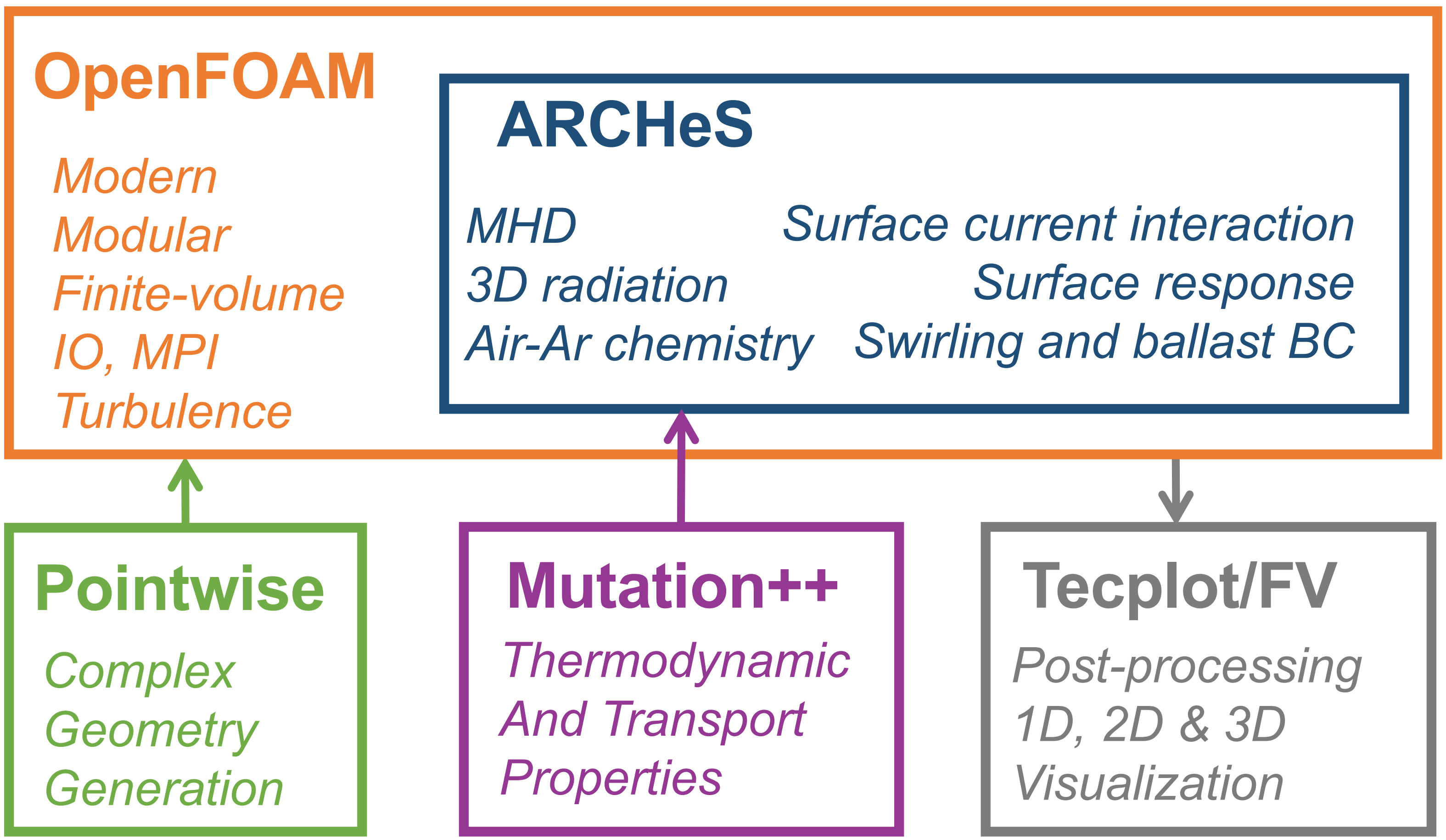

Ar-Air chemistry

$$\frac{\partial \rho_i}{\partial t} + \nabla \cdot \left(\rho_i \boldsymbol{u} + \left(\frac{\partial F_i^d}{\partial p} \right) \boldsymbol{\nabla} p + \left(\frac{\partial F_i^d}{\partial T} \right) \boldsymbol{\nabla} T + \sum_j^{N_e} \left(\frac{\partial F_i^d}{\partial Z_j^x} \right) \boldsymbol{\nabla} Z_j^x \right) = 0$$

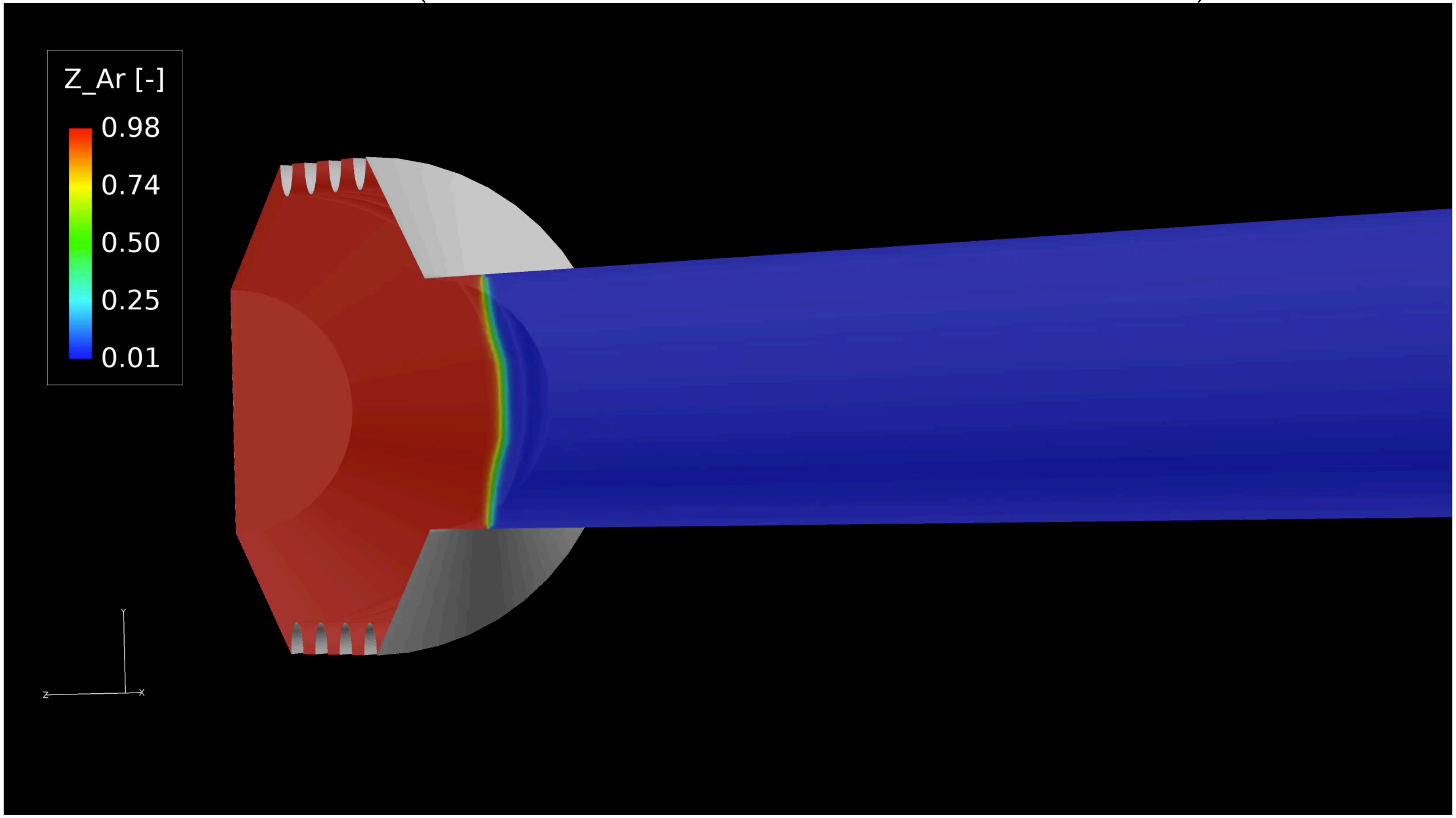

Temperature

High pressure → $T_h = T_e = T$

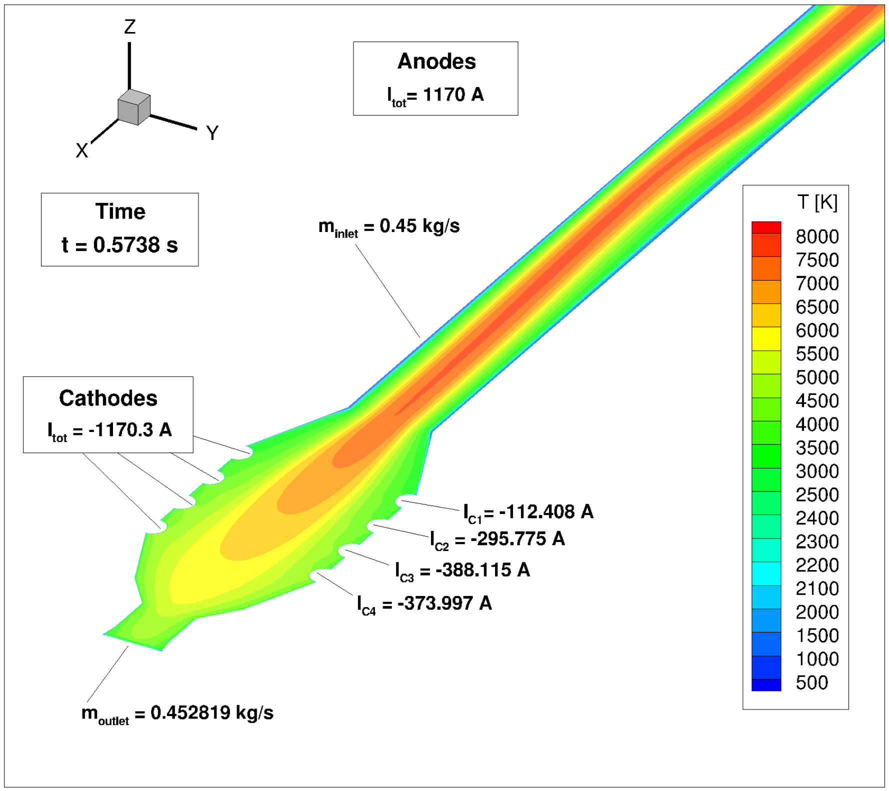

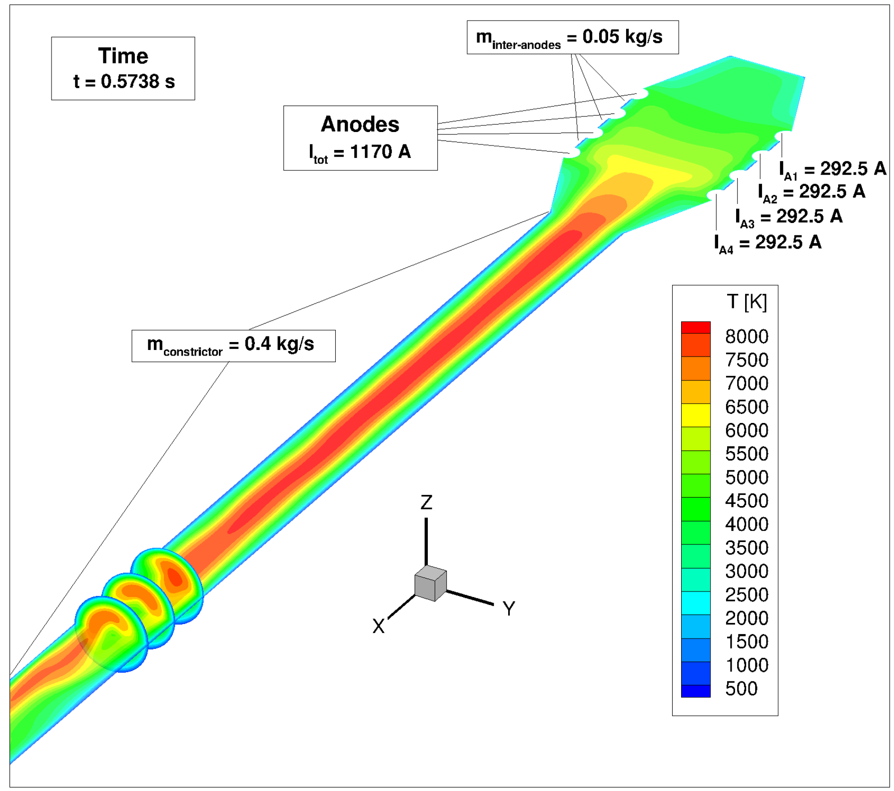

Velocity

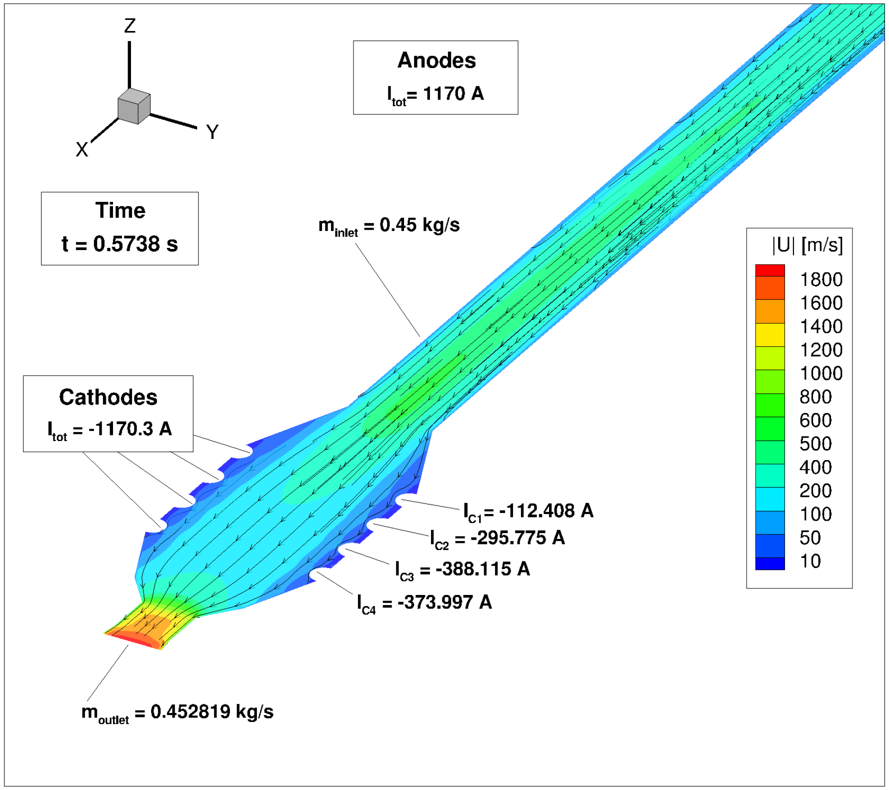
Z
Y
X
Anodes
I_{tot}= 1170 A
Time
t = 0.5738 s
m_{inlet} = 0.45 kg/s
|U| [m/s]
1800
1600
1400
1200
1000
800
600
500
400
200
100
50
10
Cathodes
I_{tot} = -1170.3 A
I_{C1}= -112.408 A
I_{C2} = -295.775 A
I_{C3} = -388.115 A
I_{C4} = -373.997 A
m_{outlet} = 0.452819 kg/s

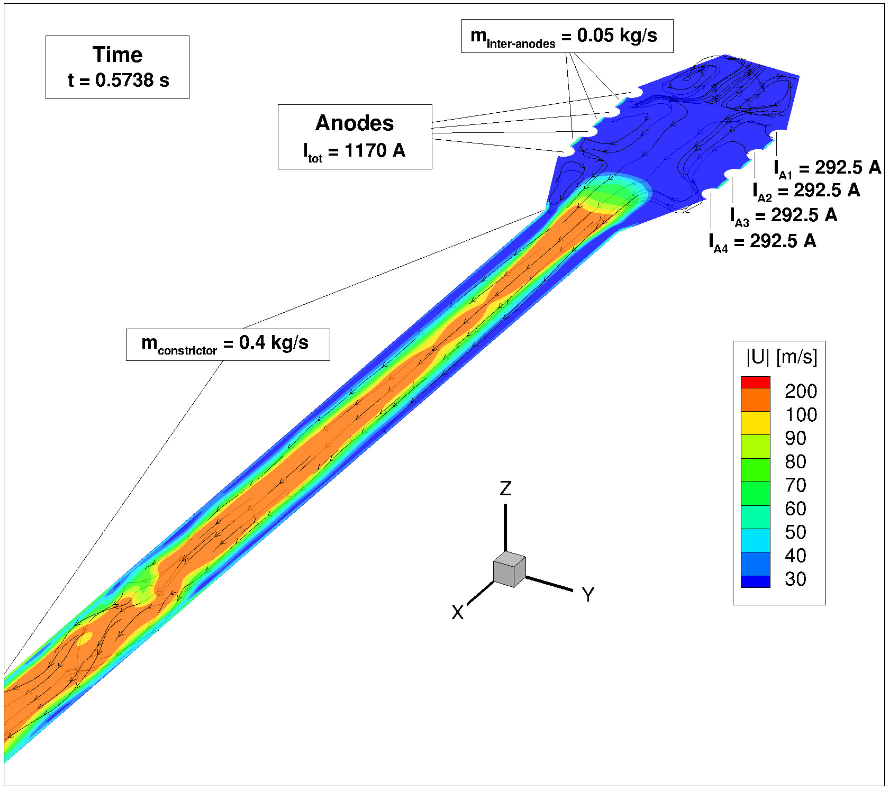
Time
t = 0.5738 s
$m_{inter-anodes}$ = 0.05 kg/s
Anodes
I_{tot} = 1170 A
I_{A1} = 292.5 A
I_{A2} = 292.5 A
I_{A3} = 292.5 A
I_{A4} = 292.5 A
$m_{constrictor}$ = 0.4 kg/s
|U| [m/s]
200
100
90
80
70
60
50
40
30
Z
Y
X

Highly unsteady and turbulent flow

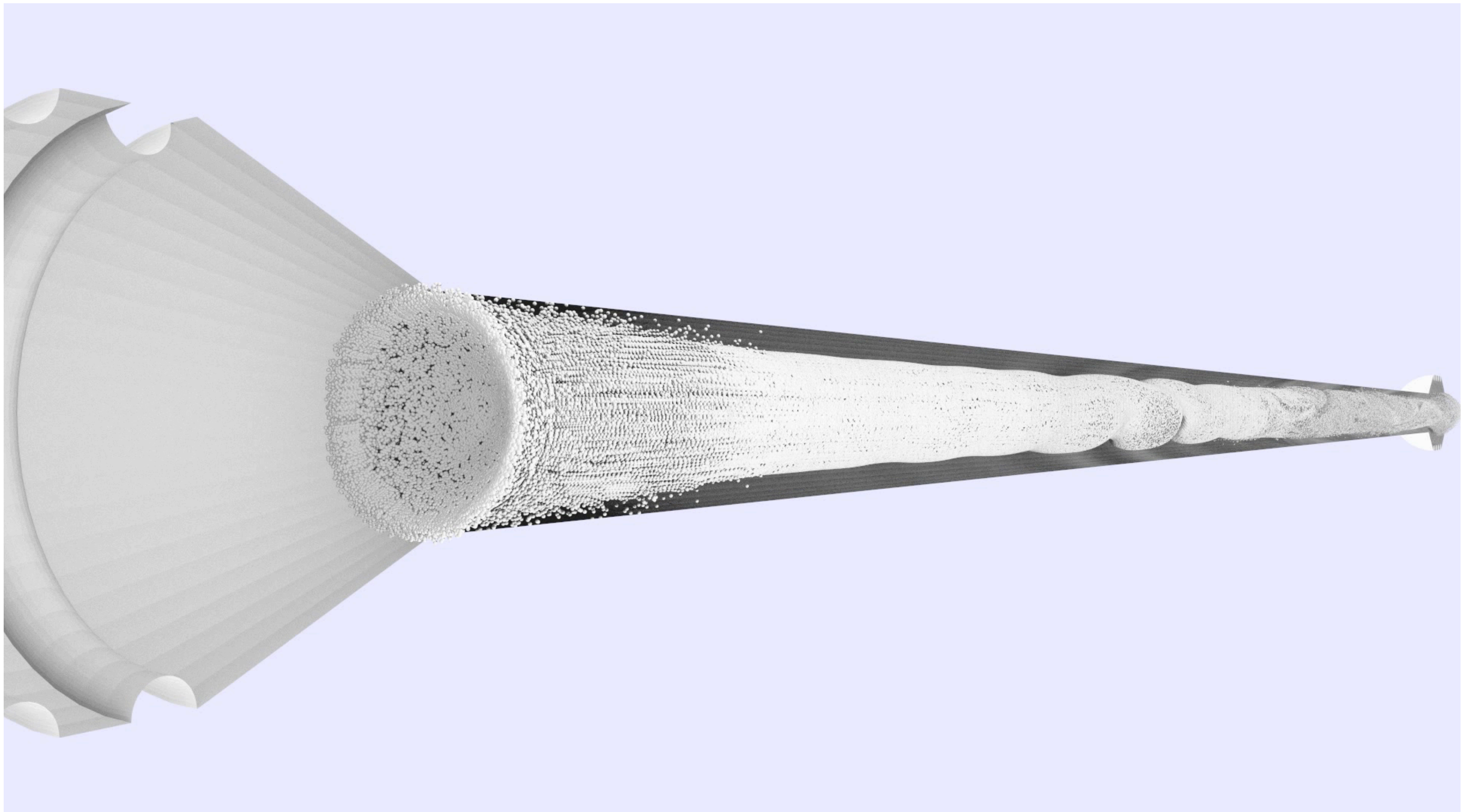

3D Radiation

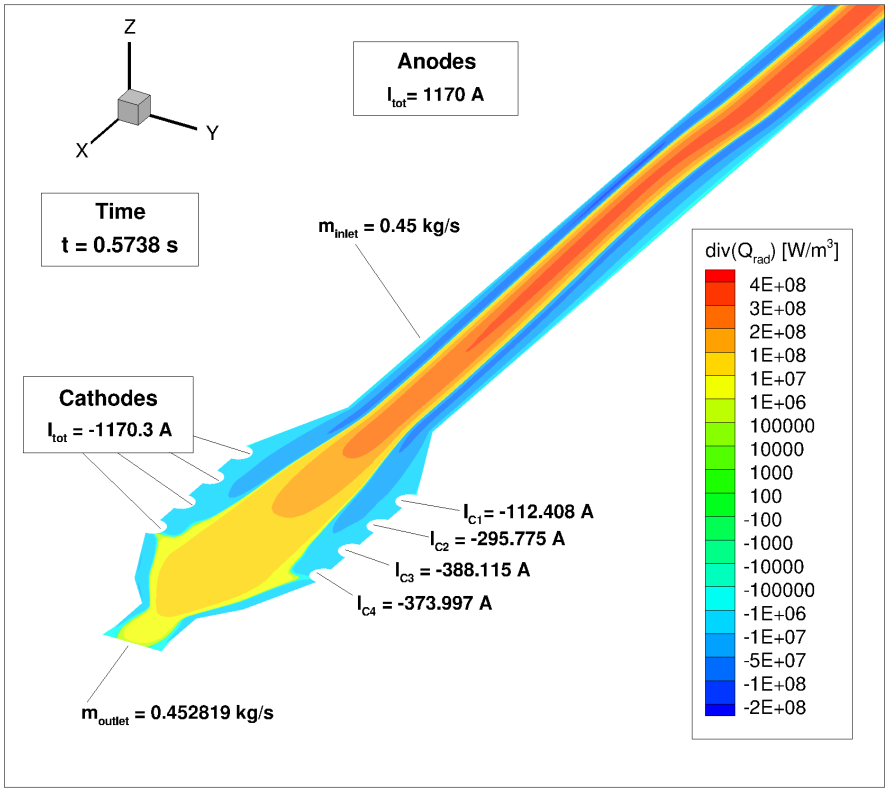

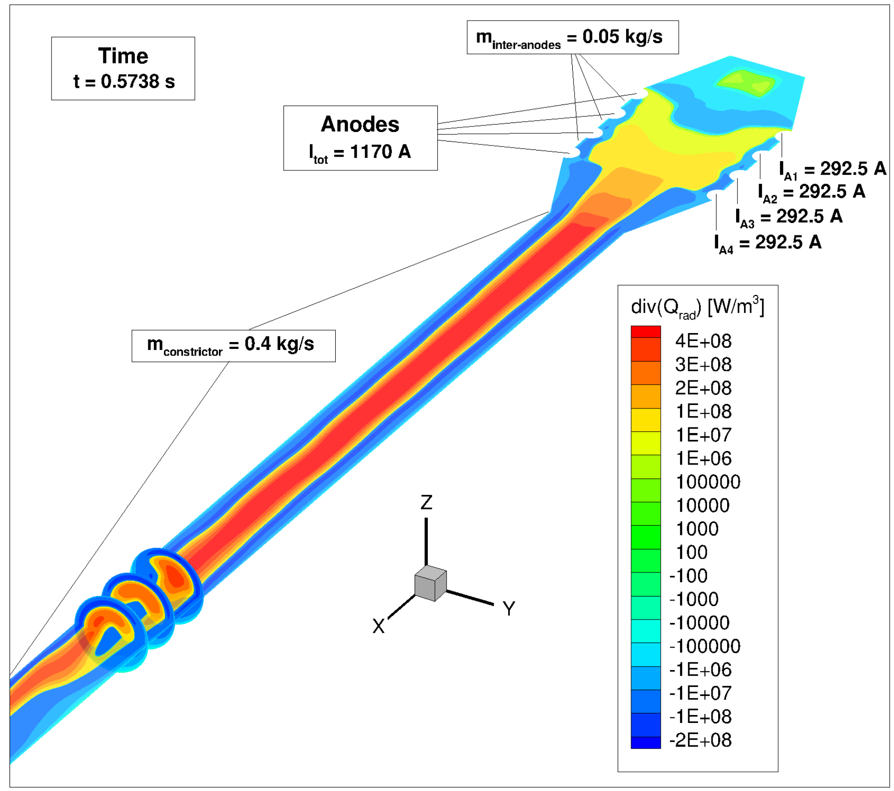

Imposed Electric Field

$$\nabla \cdot \sigma \nabla \phi = 0$$

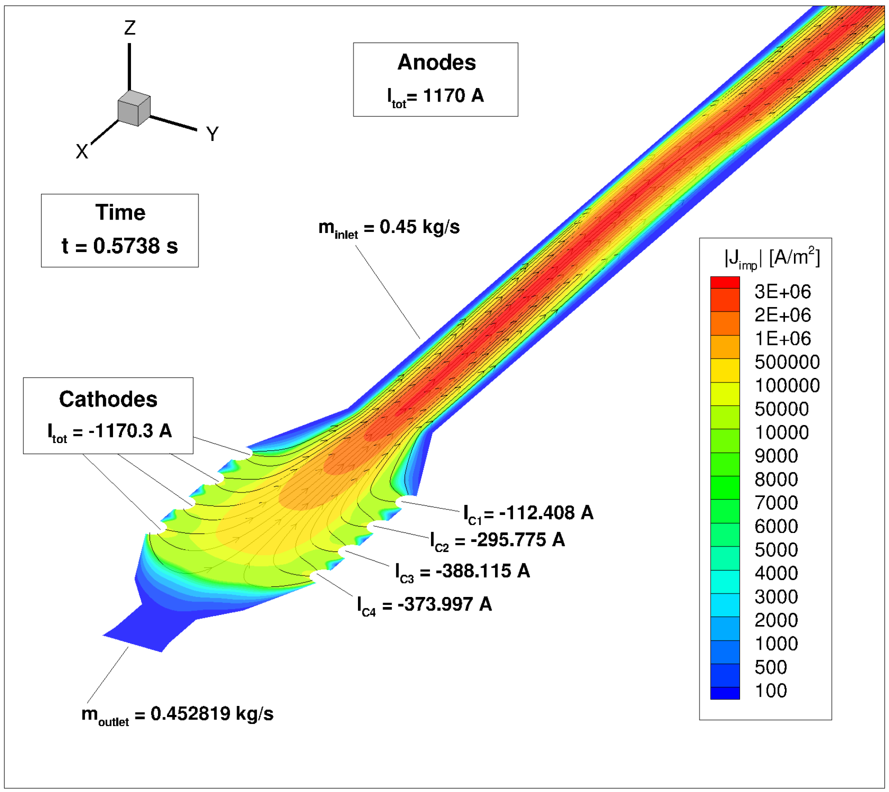

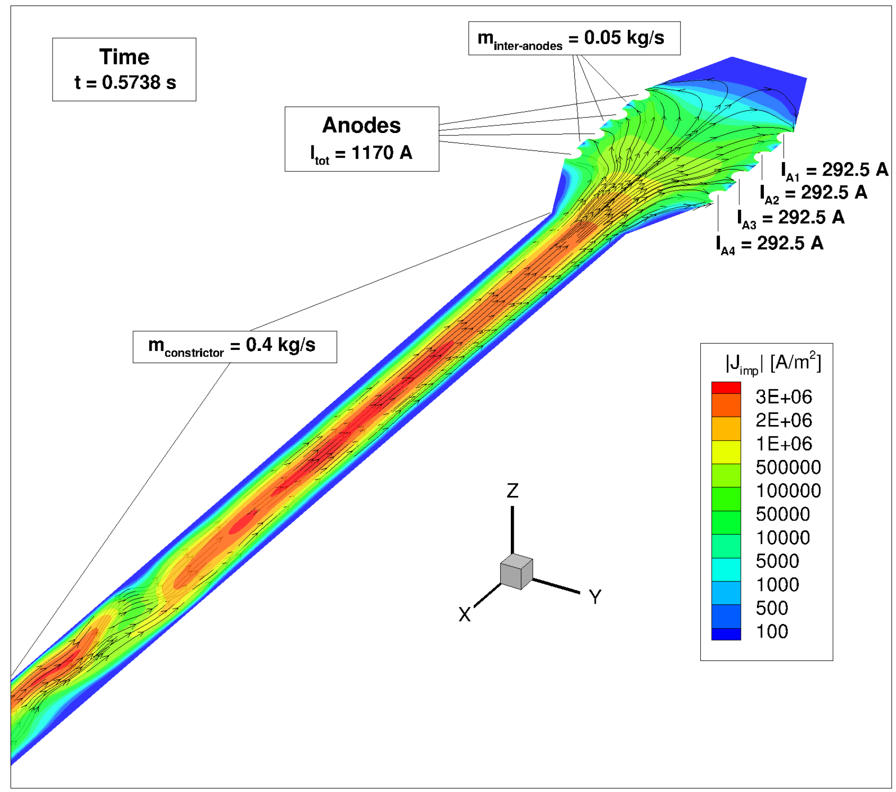

Induced Magnetic Field

$$\nabla^2 \mathbf{B} = \mu_0 \nabla\sigma \times \nabla\phi$$

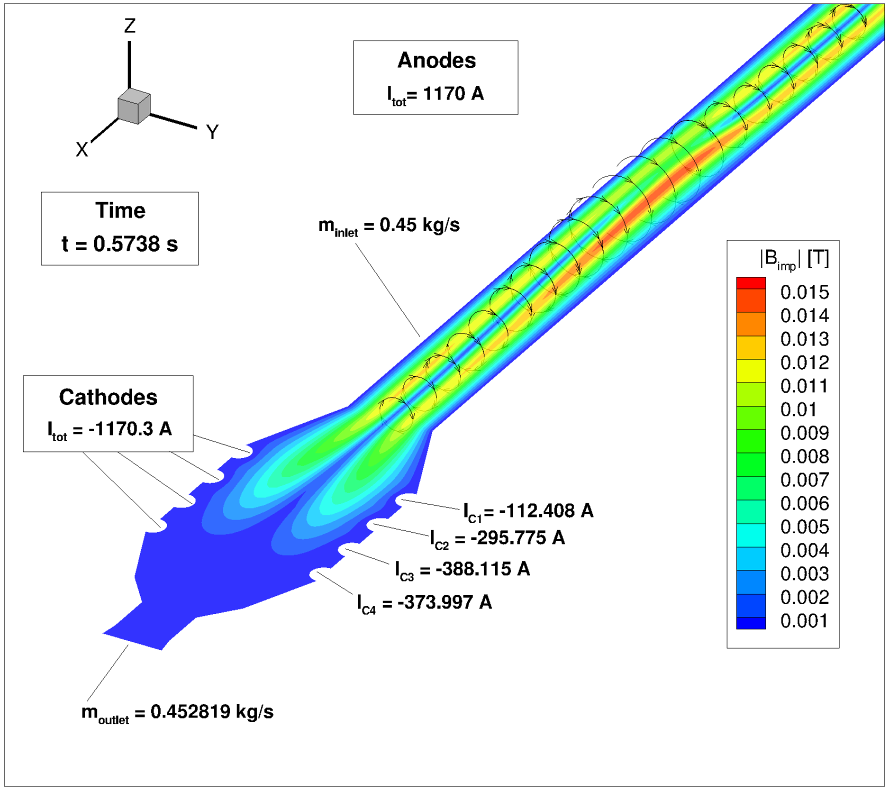

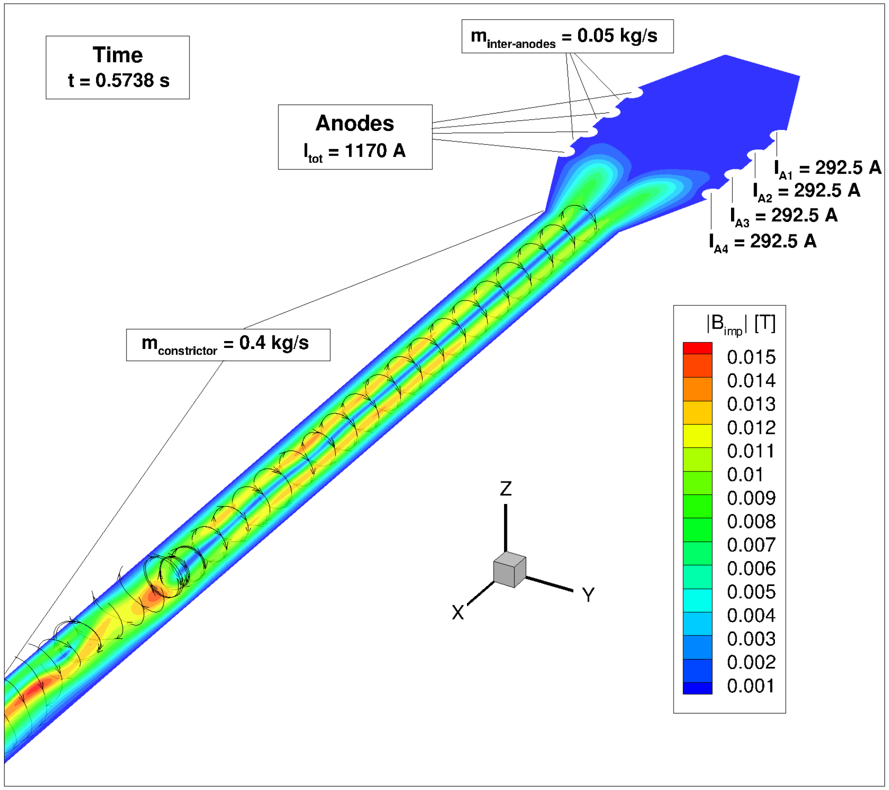

External Magnetic Field

$$\boldsymbol{B_e} = \sum_{i}^{N_e} \frac{\mu_0 I_{e_i}}{4\pi} \oint \frac{\boldsymbol{dl_i} \times \boldsymbol{r_i}}{|\boldsymbol{r_i}|^3}$$

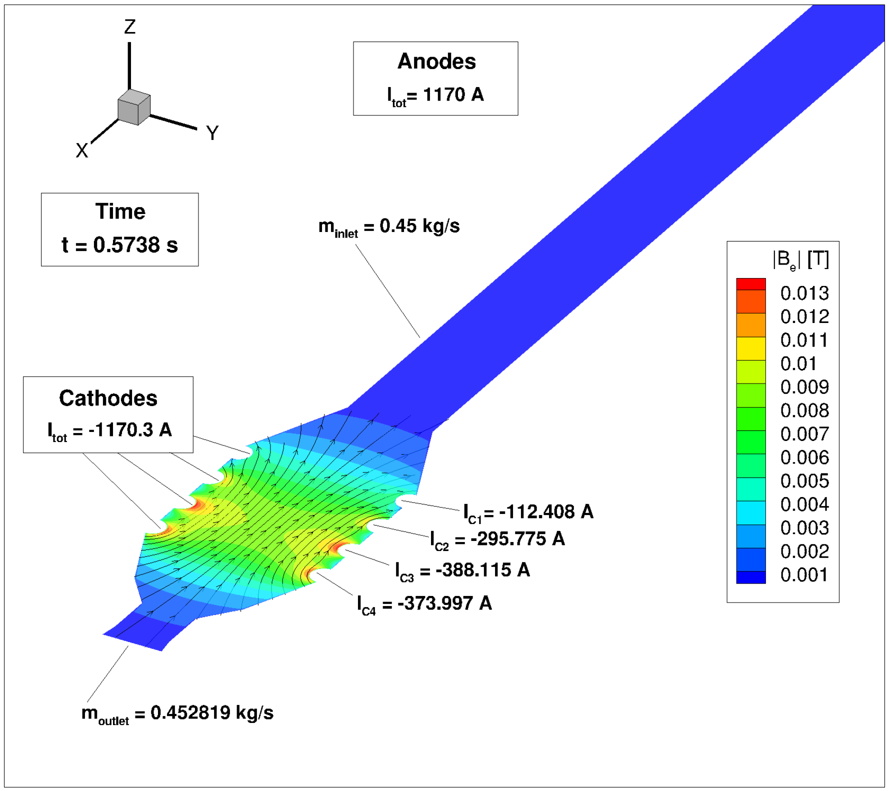

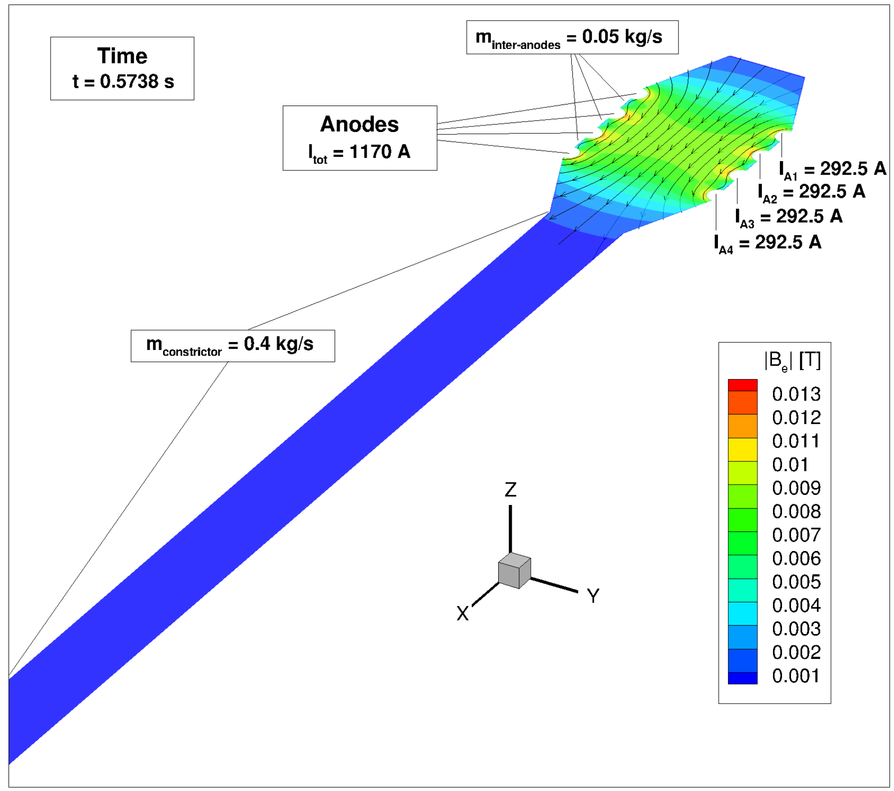

Arc instabilities in ARCHeS

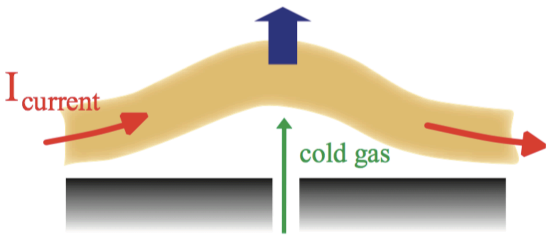

Thermal instability

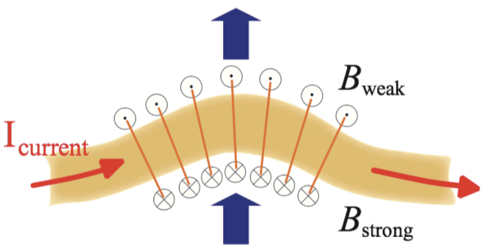

Kink instability

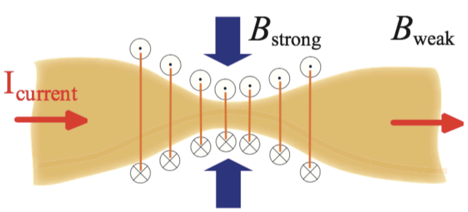

Sausage instability

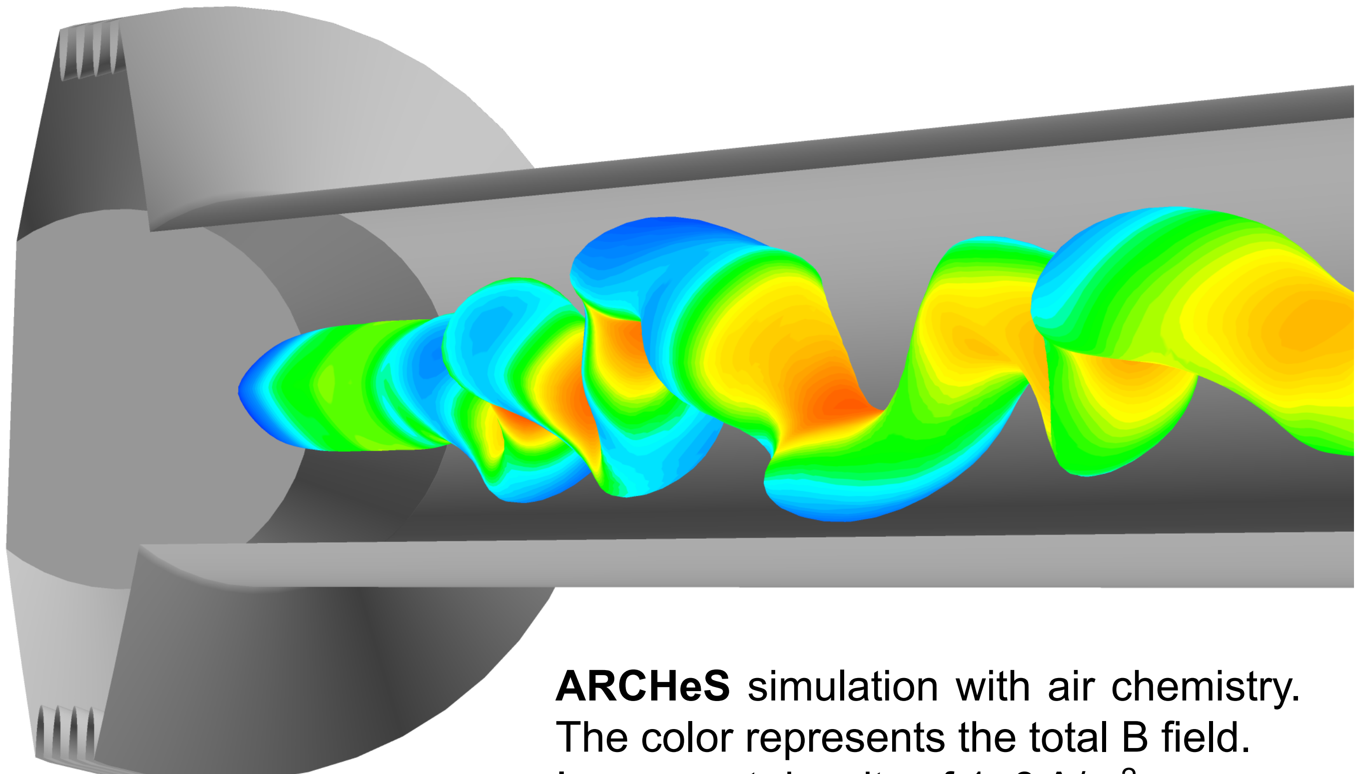

ARCHeS simulation with air chemistry.
The color represents the total B field.
Iso-current density of 1e6 A/m^2.

Arc behavior for air only

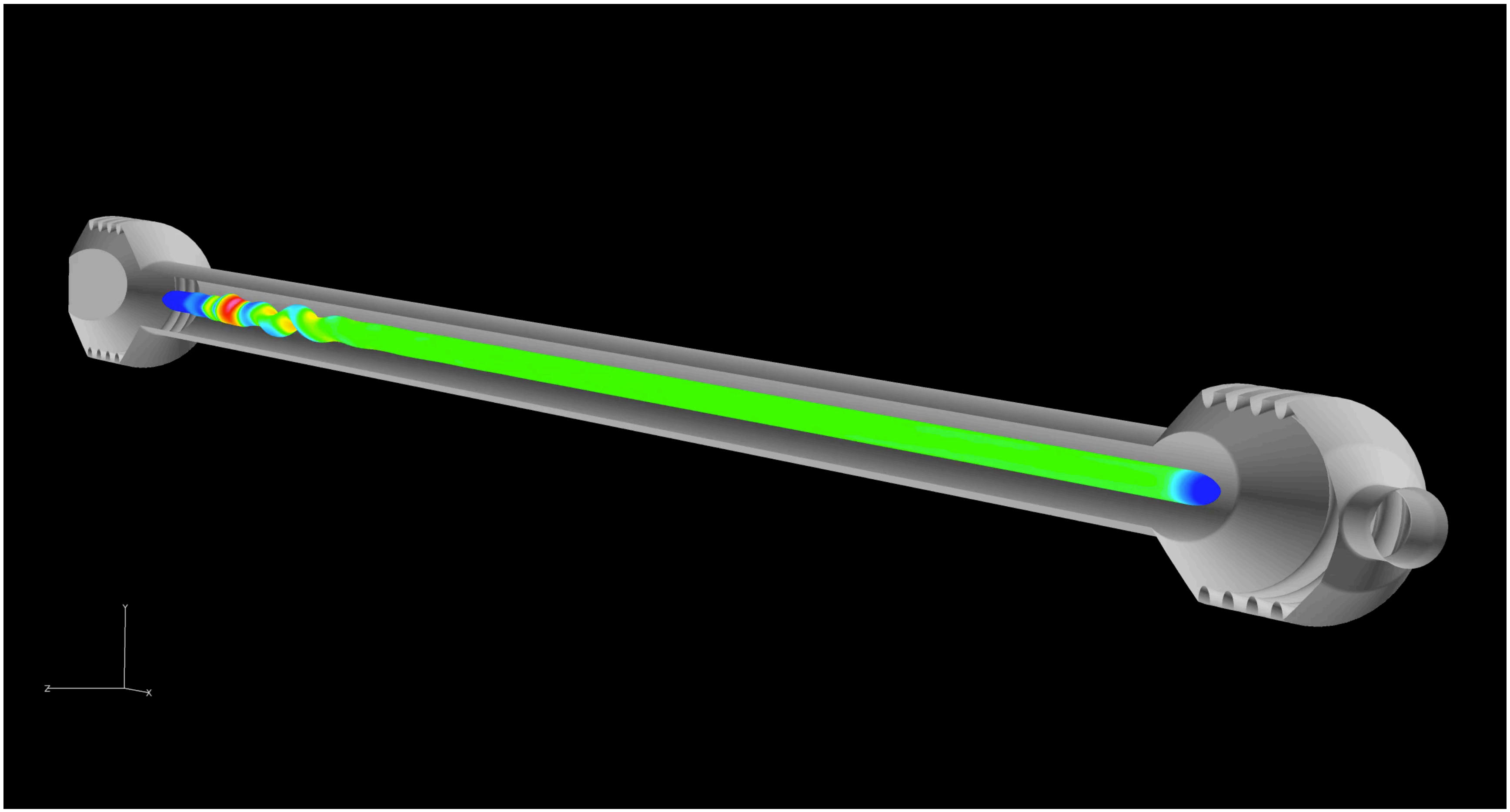

Arc behavior for air/Ar mixture

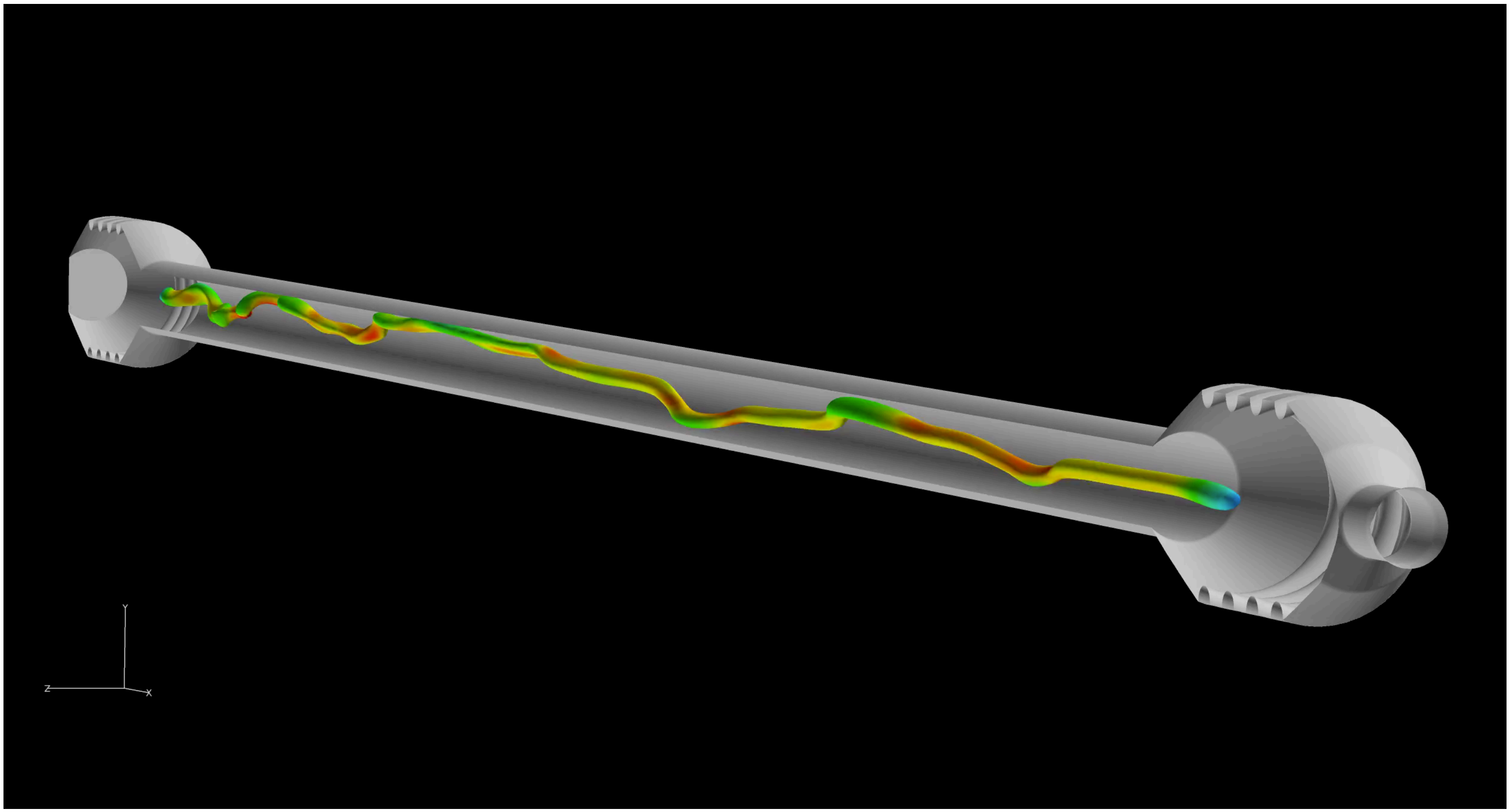

Arc reattachment

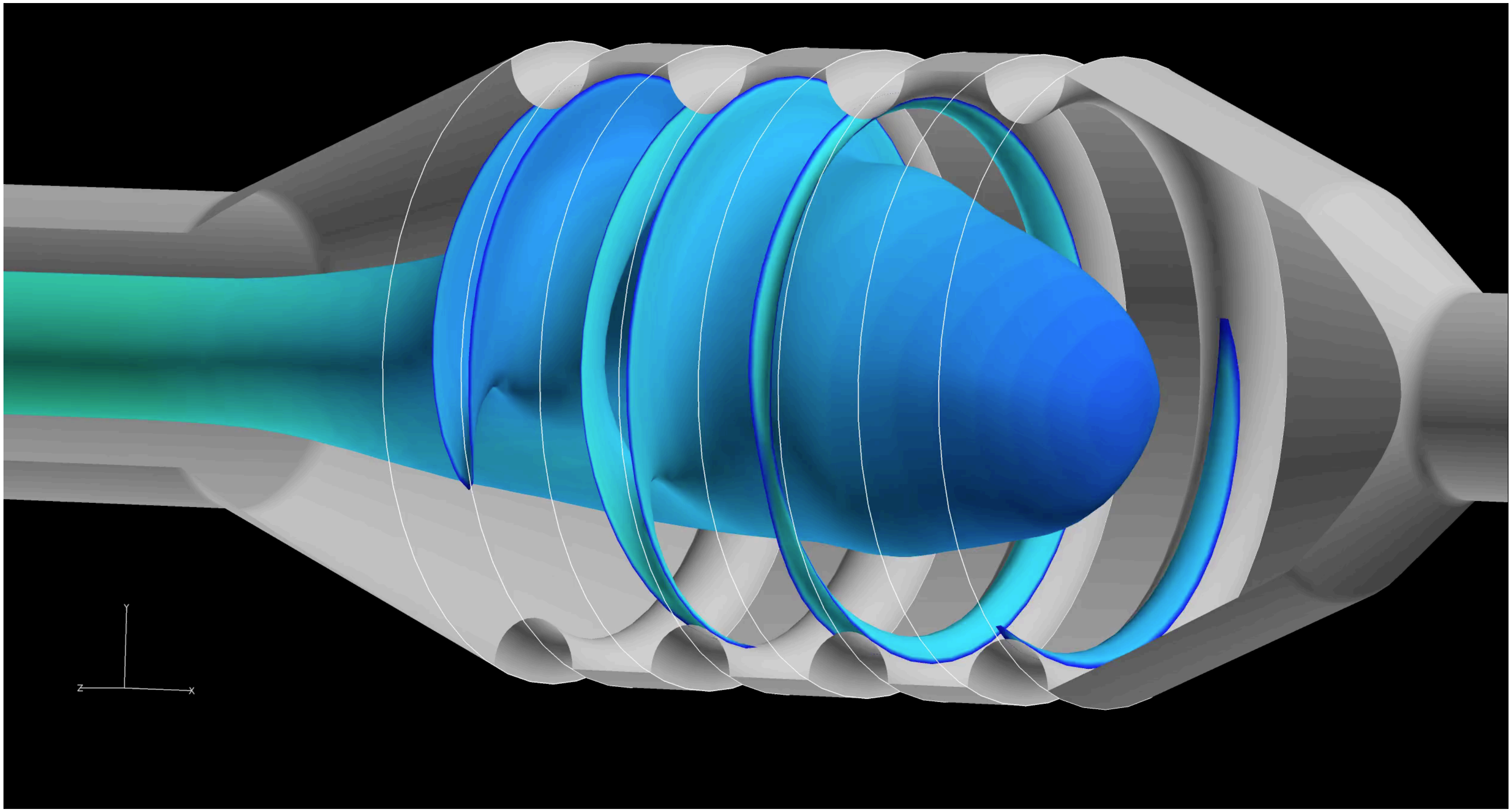

Summary

- Priority physics models have been implemented
- Working tool is being tested for:
  - Mini-ARC
  - HyMETS
  - IHF & AHF

Next Challenges

- Current numerical scheme not optimized for nearly incompressible flow – an all-speed formulation is needed
- Electrode boundary conditions
- Melt of the electrodes